Check for updates

archaeometry

Archaeometry **57**, 3 (2015) 505–535 doi: 10.1111/arcm.12077

CARGOES OF IRON SEMI-PRODUCTS RECOVERED FROM SHIPWRECKS OFF THE CARMEL COAST, ISRAEL*

E. GALILI,[1]† S. BAUVAIS,[2,4] B. ROSEN[3] and P. DILLMANN[4]

[1]*Israel Antiquities Authority and Zinman Institute of Archaeology, University of Haifa, P.O. Box 180, Atlit 30300, Israel*
[2]*CRFJ, UMIFRE 7 CNRS–MAEE (USR 3132), 3 rue Shimshon, Baka,* BP *547, Jerusalem 91004, Israel*
[3]*Israel Antiquities Authority, P.O. Box 180, Atlit 30300, Israel*
[4]*LMC–IRAMAT–CNRS (UMR 5060) and LAPA–SIS2M–CNRS–CEA (UMR 3299), Saclay, 91191 Gif-sur-Yvette Cedex, France*

Underwater surveys along the Israeli Carmel coast have revealed six cargoes of iron semi-products associated with shipwrecks. They are described and dated according to the associated artefacts. Metallographic and chemical analyses on samples from the biggest cargo have determined the stages of the chaîne opératoire*, identified the properties of the iron and characterized the iron trade along the Israeli coast. The new discoveries contribute to our understanding of the circulation of iron in the South Levant, which was characterized by an almost complete absence of local iron production. During the Byzantine and Crusader periods, this absence was compensated by long-distance sea trade, depending on political circumstances and restrictions. Three main types of iron semi-products were identified: (a) partly consolidated blooms, (b) short pointed bars and (c) elongated pointed bars. The cargoes discovered represent a time period of nearly a millennium. Altogether, 148 iron semi-products were studied. Of these, 166 were from cargo a, which was dated by coins to around 1130–1200* CE*. Those coins could have been imported from Europe for Crusader military and civil uses in the Levant. The iron from cargoes b, d and f, dated perhaps to the Byzantine period, could have been imported from Anatolia or Venice for military and civil purposes.*

KEYWORDS: IRON CARGOES, UNDERWATER ARCHAEOLOGY, CRUSADERS, BYZANTINES, SEMI-PRODUCTS

INTRODUCTION

Underwater surveys along the Israeli coast (1982–2004) have revealed numerous shipwreck assemblages, including cargoes of ancient metal ingots (Galili *et al*. 2002). This paper reports on six cargoes of iron semi-products (trade iron?), hence semi-products (see Berranger and Fluzin 2012) associated with ships wrecked off the Carmel coast (Fig. 1). The South Levant is characterized by little local iron ore reduction (Bauvais 2008). This induced long-distance trade, which was greatly influenced by changing political circumstances. Little archaeological evidence is available on the medieval sea-borne iron trade. The closest example of an iron cargo similar in character to the cargoes discussed here is reported from a 15th–16th century AD shipwreck off the Basque coast (Crew *et al*. 1997). In this paper, archaeometric studies of the semi-products were conducted on samples from cargo a, the biggest and best documented. This study contributes to our understanding of the history of the iron trade in the South Levant, and to the determination of stages in the *chaîne opératoire* (process) and characterization of the trade in iron semi-products.

*Received 26 May 2013; accepted 12 November 2013
†Corresponding author: email udi@israntique.org.il
© 2014 University of Oxford

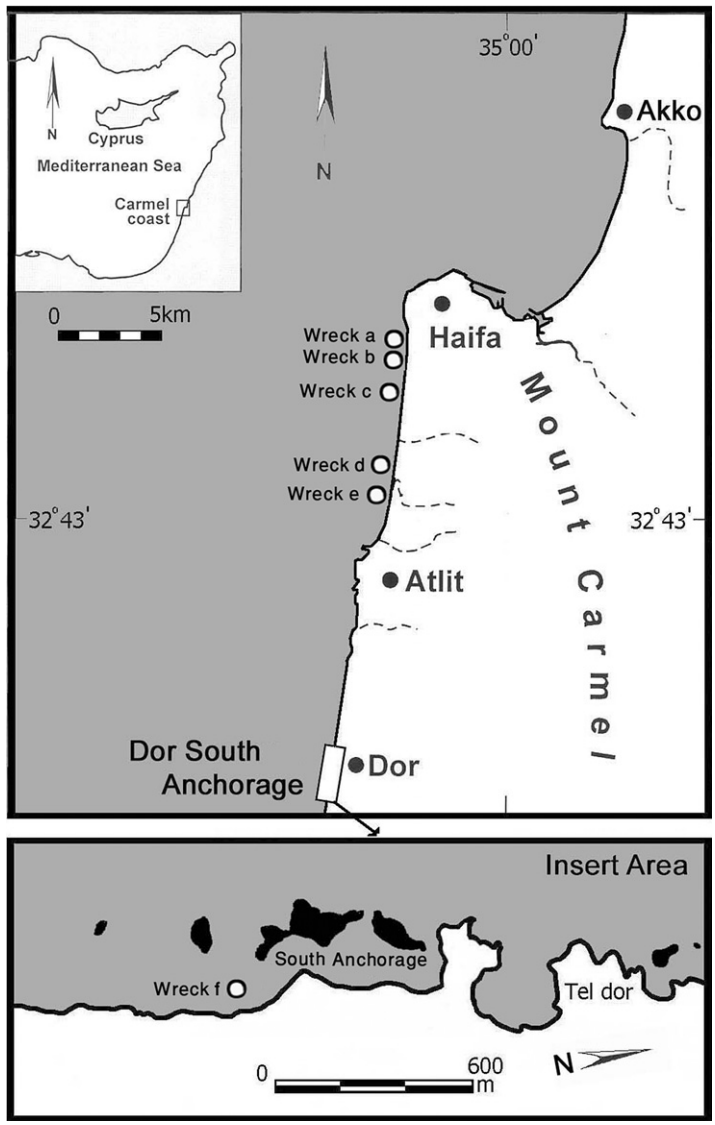

Figure 1 *The location map.*

MATERIALS AND METHODS

Archaeological fieldwork

Underwater archaeological surveys were carried out systematically after winter storms removed sandy layers covering the sea bottom, exposing archaeological sites (Galili *et al*. 2007). The semi-products were cleaned and preserved in the Israel Antiquities Authorities laboratories.[1]

[1]Supplementary items 3 and 4.

14754754, 2015, 3, Downloaded from https://onlinelibrary.wiley.com/doi/10.1111/arcm.12077 by Hanshin University, Wiley Online Library on [31/03/2026]. See the Terms and Conditions (https://onlinelibrary.wiley.com/terms-and-conditions) on Wiley Online Library for rules of use; OA articles are governed by the applicable Creative Commons License

Classification of cargo a

The dimensions of the semi-products were measured by means of calibrated tapes (±0.3 cm). Weighing was by means of a calibrated steelyard (±100 g). The typology was based on dimensional ratios, mass and shape. Discriminating indexes for separating the semi-products into classes were selected heuristically. Principal component analysis was used to divide the semi-products into typological clusters.[2] Three main types were identified. The first two of these are as follows: (a) a roughly hammered billet (hence, partly consolidated bloom) and (b) a bloom forged into a short bipyramidal double-pointed bar (hence, short pointed bar). This kind of morphology is related to technical constraints during bloom refining. For this reason, these types of semi-product can be found as far afield as the West and Central European Iron Age I (Kleeman 1961; France-Lanord 1963) and the Assyrian Iron Age, at Khorsabad or Nimrud (Pleiner and Bjorkman 1974). The third type (c) is a bloom forged into an elongated double-pointed bar (hence, elongated pointed bar). The principal component analysis of the semi-products facilitated a division between the partly consolidated blooms and the bars. Then, an agglomerative hierarchical clustering, coupled with a principal component analysis, was applied to the set of bars, revealing the two additional groups (the short pointed bar and elongated pointed bar). The partly consolidated bloom group included three types: slightly curved, trough shaped and irregular (asymmetric).

The 'chaîne opératoire' *of iron- and steel-making*

Iron- and steel-making activities can be divided into four cardinal stages (Serneels 1998; Fluzin 2001, 2002; Sauder and Williams 2002; Mangin 2004; Bauvais 2007; Bauvais and Fluzin 2009), as follows:

(1) The acquisition of raw material (ore extraction) and its preparation, including fuel (charcoal) production, an essential component of metallurgical operations.

(2) Reduction, in which the iron ore was transformed into raw metal in a shaft furnace. This combined ore, charcoal and oxygen, interacting at temperatures lower than the melting point of the metal (direct reduction). Iron and steel were collected in a pasty state, while the produced slag was liquefied. This produced a roughly compacted mass of iron or steel (bloom), containing slag and charcoal.

(3) Refining, in which the crude metal mass was compacted by heating, hammering and the agglomeration of metal fragments. Residual slag was evacuated by the welding/collapsing of initial porosities. Metal refining was by hammering, from the crude metal mass to the finished object, but it was stoppable. The product resulting at each stop was termed a 'semi-product'. Basically, the product resulting from refining is a semi-product of varying quality.

(4) The smithing phase; that is, shaping the semi-product into a product. Using various manipulations and techniques, the craftsman would achieve physical and chemical transformations. The chosen technology depended on the raw materials (quality, composition), know-how and the complexity of the final product.

Metallographic analyses

The metallographic studies were conducted according to a published protocol (Fluzin 2002; Bauvais and Fluzin 2009: see the appendix). Samples were cut, the surface finely polished (up to

[2]Supplementary items 2a–2d.

14754754, 2015, 3, Downloaded from https://onlinelibrary.wiley.com/doi/10.1111/arcm.12077 by Hanshin University, Wiley Online Library on [31/03/2026]. See the Terms and Conditions (https://onlinelibrary.wiley.com/terms-and-conditions) on Wiley Online Library for rules of use; OA articles are governed by the applicable Creative Commons License

1 μm) and the arrangement and form of the metal grains were observed microscopically. Specific reagents facilitated further observations. During reduction, the metal was produced in a (malleable) heterogeneous solid mass. Subsequent transformations (refining, thermochemical treatment, conservation conditions etc.) increased its complexity. Studied objects were sectioned, producing a large observable surface and thus achieving accuracy in texture and structure characterization. The compaction quality, or 'inclusional quality', was measured by the proportion of porosities and slag inclusions and was expressed as a percentage of the studied surface. The types and aspects of the impurities provided information concerning the fabrication techniques. Finally, using a reagent, the iron/carbon alloy composition was defined and zones differing in alloy content were localized (microstructural study).

Analyses of slag inclusions

During ore reduction, portions of the elements composing the ore are reduced, while others form a non-metallic slag. During mass compaction, some slag particles are trapped as inclusions (Ingo and Scoppio 1992). Major elements analyses tell us about the processes used to obtain the iron. The use of energy-dispersive spectrometry (EDS) combined with scanning electron microscopy (SEM) helped to distinguish the smelting systems (ore, charcoal and additives). This combination also helped us to exclude provenances (Dillmann and L'Héritier 2007) and allowed an identification of the origins of artefacts or their parts (e.g., on each side of a welded piece). A representative number of inclusions in each analysed artefact was examined. Numerous inclusions were checked to discriminate between inclusions from smelting stages and those generated by forging and fluxing agents. Using automated image analysis to detect inclusions on the metallic surfaces, spectra of between 100 and 1000 inclusions per artefact were collected. The results were expressed as the mass content of oxides: Na_2O, MgO, Al_2O_3, SiO_2, P_2O_5, K_2O, CaO, MnO and FeO. The relative precision of the measurements was about 1% for elements in concentrations better than 1% of the mass and about 10% for elements in lower concentrations. The detection limit was around 0.5 mass%. In the first step, the absolute oxides contents typical of a specific ore composition were considered: P_2O_5 and MnO. This was done after evaluating an average weighed content, accounting for the inclusion surface of each, using the formula:

$$\%E^* = \sum_{i=1}^{n} \left(\%E_i \times \frac{S_i}{S_T} \right)$$

where $\%E^*$ is the weighed content of the considered element or oxide; $\%E_i$ is the mass content of the element or the oxide in the slag inclusion (SI); S_i is the surface of the SI where the analysis was performed; S_T is the total surface of the analysed SI, and n is the total number of inclusions. This weighed content is hence indicated by an asterisk (*) (e.g., mass% P_2O_5*), to distinguish it from the measured contents. It can be converted to a pseudo-macroscopic average content and, thus, be compared with the macroscopic slag composition (Dillmann and L'Héritier 2007). To compare the contents of the non-reduced compounds (NRCs), especially MnO and P_2O_5 (to eliminate the effect of the reduction conditions in the furnace), the weighed compositions were normalized to 100% without FeO. This normalization is indicated by double asterisks (**) (Leroy *et al*. 2012). In the second step, the NRC approach was used. It was based on the fact that during smelting, MgO, Al_2O_3, SiO_2, K_2O and CaO are not reduced and conserve their respective ratios in the slag and slag inclusions. A significant observation can be made by considering four ratios, Al_2O_3/SiO_2, K_2O/CaO, MgO/Al_2O_3 and CaO/SiO_2, and only these were considered.

14754754, 2015, 3, Downloaded from https://onlinelibrary.wiley.com/doi/10.1111/arcm.12077 by Hanshin University, Wiley Online Library on [31/03/2026]. See the Terms and Conditions (https://onlinelibrary.wiley.com/terms-and-conditions) on Wiley Online Library for rules of use; OA articles are governed by the applicable Creative Commons License

Different NRC ratios between two artefacts or parts of an artefact welded together may show different systems or different origins. Similar artefacts may be obtained from the same furnace, but two smelters could generate roughly the same ratios. Only different ratios lead to definitive conclusions.

THE ARCHAEOLOGICAL FINDS

Six iron cargoes (marked a, b, c, d, e and f in Fig. 1) were found off the Carmel coast. Altogether, 148 semi-products were studied (Table 1).[3] At site a, 166 semi-products were identified and 142 were examined. Additionally, a few semi-products were salvaged from cargoes: those from cargoes b, c, d and e were examined, while others were left where found.

Cargo a: the Carmel coast

The site During 1990–8, storms exposed the seabed off the southern Haifa municipal beach (Fig. 1, a: assemblages 208 and 210 in IAA underwater survey map no. 7). The site lies some 60–80 m offshore, at a depth of 2.8 m. Remains dated to the 12th century CE, associated with the semi-products, are discussed here (Galili and Sharvit 1999a,b; Galili *et al*. 2002, 2010). Prior to modern construction work, the shoreline was open, sandy and straight, orientated on a north–south axis. The sea bottom is composed of sand over hard, fossil clay. The organic parts of the ship and the cargo had vanished. The remaining artefacts were lying on the clay over an area measuring 40×30 m and formed a single recognizable shipwreck site.

Iron nails Twenty-one iron nails in different states of preservation were retrieved (Fig. 2). They had a rectangular cross-section (10×10 mm) shaft (120–135 mm long) and a round, slightly conical, flat head (25 mm in diameter). Most (17) were scattered on the sea bottom, while four were attached to the semi-products. Fifteen nails were complete and six were headless shafts. A few were attached to plant fibres, probably to prevent water leakage by sealing nail holes. They probably joined planking to frames, as planking requires a relatively large number of nails. Judging by the size of the nails, the vessel was of a medium size (12–17 m long).

The semi-products Altogether, 166 semi-products were recovered and 142 were studied (Table 1). They formed three sub-clusters: A, 93 partly consolidated blooms; B, 19 short pointed bars; and C, 30 elongated pointed bars. The additional semi-products that are not included in this study consist of one elongated bar, one short pointed bar and 22 partly consolidated blooms. After cleaning, the weight of the 93 studied partly consolidated blooms was 974.5 kg (average 10.2 kg), the 19 short pointed bars weighed 42.4 kg (average 2.23 kg) and the weight of the 30 elongated pointed bars was 56.9 kg (average weight 1.9 kg). The total weight of the semi-products in this assemblage was 1073.8 kg. Assuming the same proportion and same average masses, the iron cargo weighed about 1300 kg. The semi-products were concentrated in a relatively small area (10×5 m). They had probably stayed in the same location on the seabed since the shipwreck, thus representing the original arrangement of the cargo. The partly consolidated blooms were joined by concretion into a disorganized pile, while the elongated pointed bars were in groups of 15–20 specimens attached alongside. Perhaps they were bound by circumscribing perishable bands or laid in plant fibre containers. Traces of fibres (palm fronds?), mats or baskets were still visible on some of the semi-products when found.

[3]See also Supplementary item 1.

14754754, 2015, 3, Downloaded from https://onlinelibrary.wiley.com/doi/10.1111/arcm.12077 by Hanshin University, Wiley Online Library on [31/03/2026]. See the Terms and Conditions (https://onlinelibrary.wiley.com/terms-and-conditions) on Wiley Online Library for rules of use; OA articles are governed by the applicable Creative Commons License

Table 1 *The properties of the iron cargoes*

Assemblage	*Average length of semi-product (cm)*	*Total weight of iron cargo*	*Total weight of studied semi-product and average weight (kg)*	*Type of semi-product*	*Number of studied semi-products*	*Number of semi-products*	*Period*	*Site*
a	30		974.5 (10.2)	Partly consolidated bloom	93	115	12th century CE Crusader period	Carmel coast
a	32.5		42.45 (2.23)	Short pointed bar	19	20	As above	As above
a	47.3		56.9 (1.9)	Elongated pointed bar	30	31	As above	As above
Total for assemblage a	–	1302	1074	–	142	166	As above	As above
b	45–50	350	–	Partly consolidated bloom/short pointed bar	–	35	Byzantine	Hishuley Carmel
c	28	200	16	Partly consolidated bloom	1	15	15th–18th centuries CE?	Kfar Galim
d	28	208	16	Partly consolidated bloom	1	13	Roman/Byzantine/ Early Islamic?	Tel Hreiz
e	28	1700	8.6	Partly consolidated bloom	1	~200	Late medieval	Tel Qar'a
f	31	100	56.2 (18.7)	Partly consolidated bloom	3	7	Byzantine	Dor, south bay

© 2014 University of Oxford.

14754754, 2015, 3, Downloaded from https://onlinelibrary.wiley.com/doi/10.1111/arcm.12077 by Hamslin University, Wiley Online Library on [31/03/2026]. See the Terms and Conditions (https://onlinelibrary.wiley.com/terms-and-conditions) on Wiley Online Library for rules of use; OA articles are governed by the applicable Creative Commons License

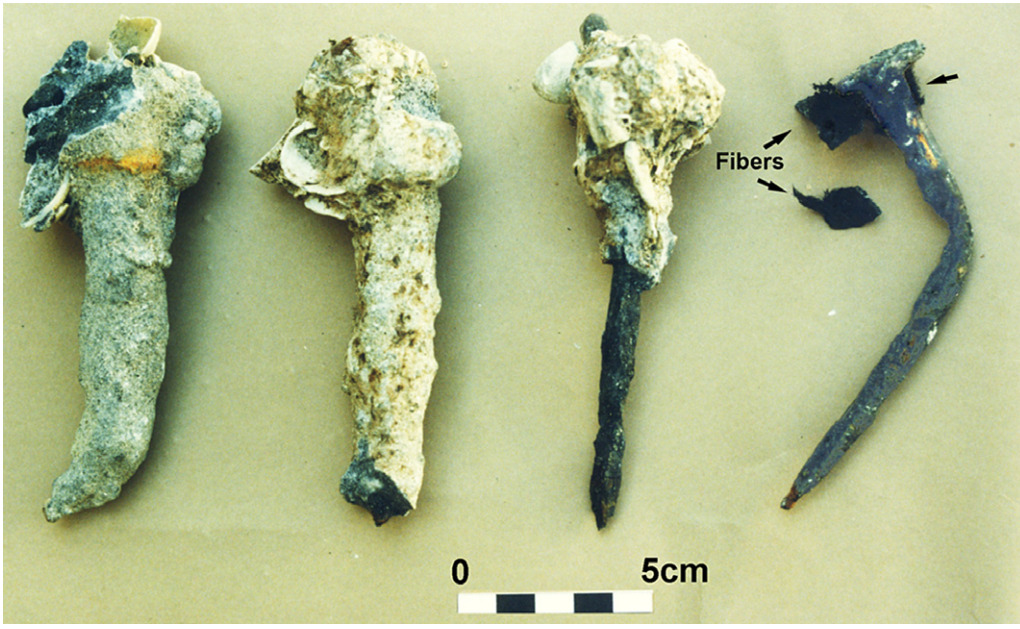

Figure 2 *Iron nails from assemblage a.*

Type A—partly consolidated blooms. These semi-products were crudely worked (Fig. 3, right). Some semi-products showed signs of slag removal and volume reduction by hammering and compression of voids. Of such rectangular semi-products, 115 were recovered and 93 are discussed. They were roughly divided into three subtypes: slightly curved, trough shaped and irregular/asymmetric.

Type B—short pointed bars. These semi-products are elongated, symmetric and well-shaped, with tapered pointed ends, and their proportions and weights vary (Fig. 4, bottom). Twenty were recovered and 19 are listed in Table 1. They are generally more carefully formed than the partly consolidated blooms. One showed parallel-crossing depressions left by forging. One semi-product showed three incised, chiselled lines (Fig. 4, top).

Type C—elongated pointed bars. These semi-products (Fig. 4, centre) are similar to the short pointed bars but are thinner and longer. The short pointed bars and the elongated pointed bars are usually symmetrical and well-shaped, often having tapered pointed ends. Thirty-one elongated pointed bars were recovered and 30 are listed in Table 1. Some possess parallel-crossing depressions left by forging.

Coins Nine sections of gold coins cut by a chisel were found (Fig. 5), most laid 10–15 m south-east of the main concentration of semi-products. These were Crusader coins, most from the mid-12th century CE (R. Kool pers. comm. 2010). Judging by the coins, the shipwreck occurred during the 12th century.

The context Adjacent to the semi-products were an iron hammer, a caulking iron (Fig. 6) and an iron sickle with a wooden handle. They may have been part of toolkits belonging to the ship's carpenter or the boatswain.

14754754, 2015, 3, Downloaded from https://onlinelibrary.wiley.com/doi/10.1111/arcm.12077 by Hanshin University, Wiley Online Library on [31/03/2026]. See the Terms and Conditions (https://onlinelibrary.wiley.com/terms-and-conditions) on Wiley Online Library for rules of use; OA articles are governed by the applicable Creative Commons License

Figure 3 *A pile of semi-products from cargo a.*

Cargo b: Hishuley Carmel

The site lies a few hundred metres south of the Haifa municipal beaches, some 60–100 m offshore, at a depth of 3–5 m (Fig. 1, b). The shoreline is like that of site a. The semi-products were scattered over an area measuring 40 × 20 m, at a depth of 4–5 m. A concentration of five Byzantine iron anchors was found 50–60 m south-east of the semi-products, probably representing the ship carrying them.

The semi-products The 35 semi-products were documented on the sea bottom. They were shaped into elongated partly consolidated blooms, measuring about 45 × 10 × 8 cm and weighing about 7–12 kg each. The whole cargo of semi-products weighed about 350 kg.

Context Five iron anchors and four anchor stocks found in 1987 (Fig. 7) were scattered over an area of 16 × 6 m area, at a water depth of 2.4–2.6 m. A smaller anchor, with its stock in a working position, was some 35 m to the north-west, at a water depth of 2.8 m. It probably functioned as a working anchor during the shipwreck event. The others were reserve anchors stored on-board. Such anchors (type D—Kapitan 1984) were used during the fifth to eighth centuries CE (Galili and Rosen 2008a,b). Thus the shipwreck may be dated to the Byzantine period.

Cargo c: Kfar Galim

The site lies some 1500 m south of the Haifa municipal beaches, some 60–100 m offshore, at a depth of 3–4 m (Fig 1, c). The seabed and the shoreline are like those of site a. The semi-products were scattered over an area measuring 60 × 20 m on the clayish seabed, at a depth of 3–4 m.

14754754, 2015, 3, Downloaded from https://onlinelibrary.wiley.com/doi/10.1111/arcm.12077 by Hanshin University, Wiley Online Library on [31/03/2026]. See the Terms and Conditions (https://onlinelibrary.wiley.com/terms-and-conditions) on Wiley Online Library for rules of use; OA articles are governed by the applicable Creative Commons License

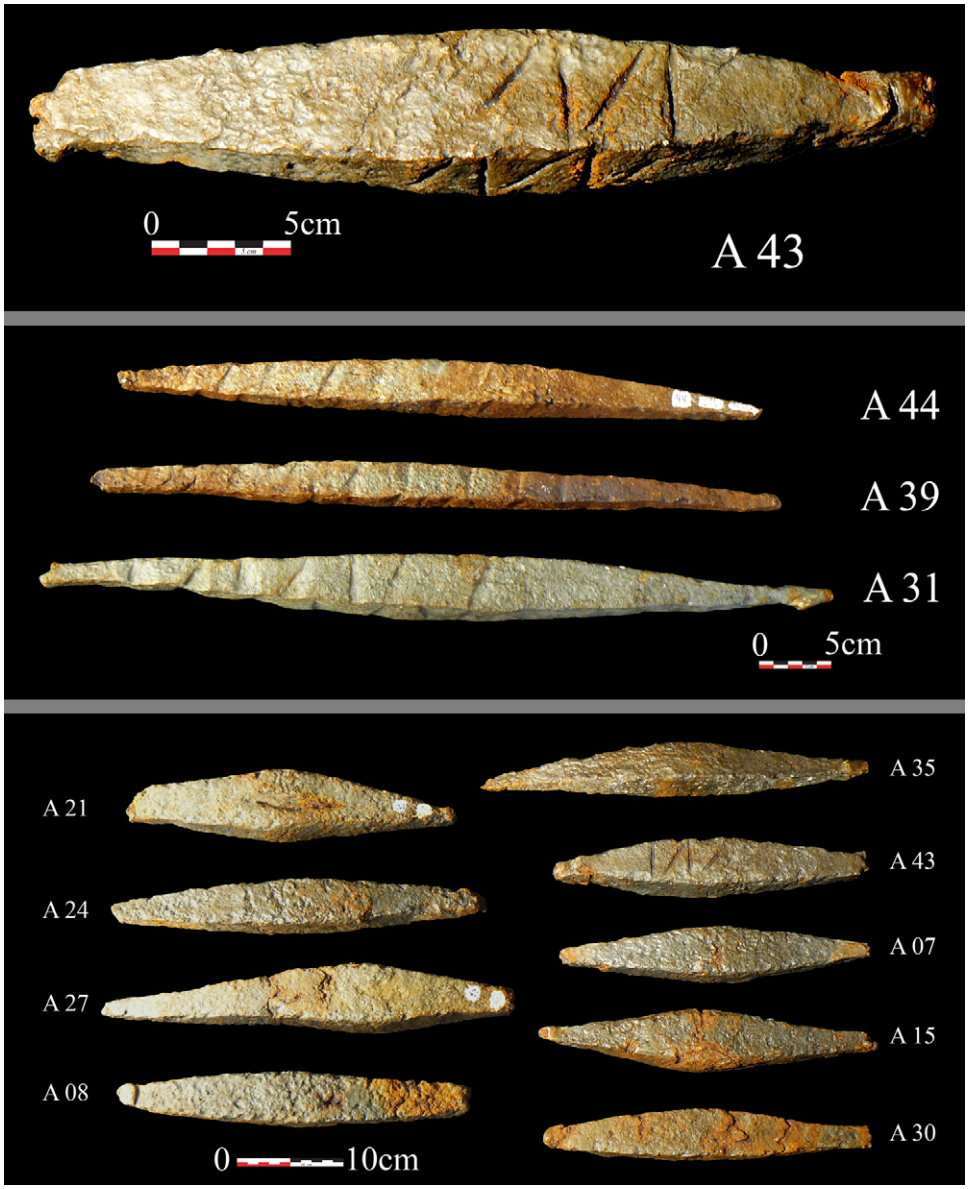

Figure 4 *Semi-products from cargo a: top, chisel signs (incisions); middle, elongated pointed bars; bottom, short pointed bar.*

The semi-products Fifteen partly consolidated blooms were found on site; two were retrieved and one was studied. It weighs 13.6 kg and is 33 cm long. The whole cargo of semi-products weighed about 200 kg.

The context Two Byzantine iron anchors and a shipwreck assemblage, dated to the medieval period, were observed near the semi-products. Two iron cannons retrieved by a

14754754, 2015, 3, Downloaded from https://onlinelibrary.wiley.com/doi/10.1111/arcm.12077 by Hanshin University, Wiley Online Library on [31/03/2026]. See the Terms and Conditions (https://onlinelibrary.wiley.com/terms-and-conditions) on Wiley Online Library for rules of use; OA articles are governed by the applicable Creative Commons License

Figure 5 *Slices of 12th-century gold coins cut by a chisel.*

fisherman were sold before documentation. The semi-products may be dated to the 15th–18th centuries CE.

Cargo d: Tel Hreiz

The site is located 5.5 km south of Haifa, some 60–100 m offshore, at a depth of 3–4 m (Fig. 1, d). It is similar to site a. The artefacts were scattered over an area measuring 60 × 40 m. The site included artefacts from the Roman, Byzantine and early Islamic periods. The semi-products may be associated with any of these eras.

The semi-products Thirteen partly consolidated blooms, similar in shape and weight, were scattered on the sea bottom. One was retrieved and documented: it weighs 16 kg and is 28 cm long (Table 1). The whole cargo weighed about 208 kg.

Cargo e: Tel Qar`a

The site (30 × 30 m) which lies 50–60 m offshore at a depth of 2.0–2.5 m (Fig. 1, e) is similar to site a.

14754754, 2015, 3, Downloaded from https://onlinelibrary.wiley.com/doi/10.1111/arcm.12077 by Hanshin University, Wiley Online Library on [31/03/2026]. See the Terms and Conditions (https://onlinelibrary.wiley.com/terms-and-conditions) on Wiley Online Library for rules of use; OA articles are governed by the applicable Creative Commons License

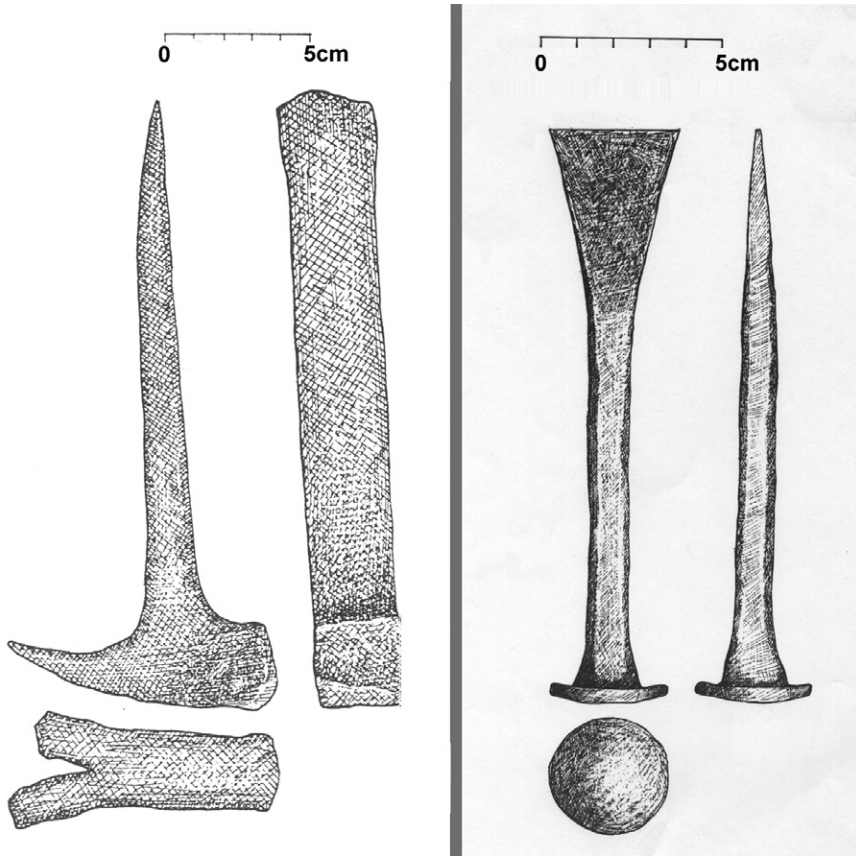

Figure 6 *Left, an iron hammer; right, an iron caulking tool.*

The semi-products A pile of semi-products, roughly $1.5 \times 1.5 \times 0.5$ m, contained about 200 partly consolidated blooms. One was retrieved and documented: it weighed 8.6 kg and was 28 cm long (Table 1). The whole cargo weighed about 1700 kg.

The context Two stockless iron anchors about 3 m long, weighing some 300 kg each, were laid 3 m apart in relatively shallow water, near the semi-products. They belonged to a medium-to-large vessel (20–30 m long) and were used from late medieval to pre-modern times. The shipwreck may be dated to the 15th–18th centuries CE.

Cargo f: Dor south anchorage

The Dor south anchorage is one of the best-protected natural shelters along the Israeli coast (Fig. 1, f). The site has been inhabited intermittently at least since 2000 BC. It is protected from the west by a sandstone ridge. The wreckage lies in the anchorage, about 60 m offshore, at a depth of 2.5–3.5 m (Fig. 1, f), covering an area measuring 15×25 m (Galili *et al*. 2007; Galili and Rosen 2008a).

14754754, 2015, 3, Downloaded from https://onlinelibrary.wiley.com/doi/10.1111/arcm.12077 by Hanshin University, Wiley Online Library on [31/03/2026]. See the Terms and Conditions (https://onlinelibrary.wiley.com/terms-and-conditions) on Wiley Online Library for rules of use; OA articles are governed by the applicable Creative Commons License

Figure 7 *Byzantine iron anchors from assemblage b.*

The semi-products Seven partly consolidated blooms were recovered some 25 m south-west of the wreckage (Fig. 8). They weigh 13.4–23 kg and are 30–33 cm long (Table 1). The whole cargo weighed about 130 kg.

The context The assemblage included ashlar sandstones, fishing gear and the bronze counterweight of a steelyard, in the shape of a female bust.[4] Numerous square-sectioned iron nails, 13–21 cm long, represented the hull. Iron tools included an axe, a builder's hammer and a drill (Galili and Rosen 2008a).

Coins The coins (Fig. 9) were minted from the reign of Anastasius I (AD 498–518) to that of Constantine II (AD 641–668), the latest dated to AD 659–663/4. The wreck must have occurred not much later than AD 665 (Syon and Galili 2009).

The ship According to the nails, it was a medium-sized vessel. The fishing gear indicates trading augmented by fishing.

ARCHAEOMETRIC RESULTS

Three semi-products from cargo a, the partly consolidated bloom A108, the short pointed bar A047 and the elongated pointed bar A004, were studied using the analytical protocol (see the appendix). The qualitative results, complemented by a quantitative study, provide statistical data for detailed interpretations.

[4]Supplementary item 5.

14754754, 2015, 3, Downloaded from https://onlinelibrary.wiley.com/doi/10.1111/arcm.12077 by Hanshin University, Wiley Online Library on [31/03/2026]. See the Terms and Conditions (https://onlinelibrary.wiley.com/terms-and-conditions) on Wiley Online Library for rules of use; OA articles are governed by the applicable Creative Commons License

Figure 8 *A diver examining partly consolidated blooms from cargo f.*

Metallography

Partly consolidated bloom A108 This is a massive, slightly curved block (A1), weighing 7.1 kg. It is 25.5 cm long, 12 cm wide and 7 cm thick. The longest sides were hammered and the top surface has several folds (Fig. 10). The cross-section surface, made transversely, is heterogeneous, having large pores surrounded by slag in the centre and at both extremities (Fig. 11). One of the two long sides is composed mainly of slag, in which prills and metallic filaments are distributed. The other side is much denser, with small inclusions in a compact metal mass. The two section ends are less densified, containing wide zones of slag and curved metal lines that sometimes form what could be negatives of ore grains. Generally, this partly consolidated bloom demonstrates poor inclusion cleaning, with an inclusion rate of 28.8% of the cut surface (Fig. 11). Metallographic analysis confirms the heterogeneity of the cut surface and allows its characterization. In the less-densified parts, which contain much of the slag (fayalite with dendrite and globules of wüstite), the metal shows little deformation after reduction. Metal prills are perfectly round (Fig. 12, 003/006/015) and most metal bands coalesced in the outlines of partially reduced ore grains (Fig. 12, 004/007/012). In areas of denser metal, the inclusions are deformed and flattened, implying a hammering of the parallel adjacent surface (Fig. 12, 005/014/018). Between the two cases mentioned above, there is a progression, which enables us to follow the inclusions and deformation of metal grains, as well as slag evacuation (Fig. 12, 008/011/017). Nital etching shows that the metal is 97.2% ferrite (0.02% C) (Fig. 12, 021/023). In a few places, a slight carburization, of up to 0.4% carbon, is seen (Fig. 12, 020/025). This metal mass presents a well-compacted area, close to the most flattened surface, indicating hammering from this surface.

14754754, 2015, 3, Downloaded from https://onlinelibrary.wiley.com/doi/10.1111/arcm.12077 by Hanshin University, Wiley Online Library on [31/03/2026]. See the Terms and Conditions (https://onlinelibrary.wiley.com/terms-and-conditions) on Wiley Online Library for rules of use; OA articles are governed by the applicable Creative Commons License

Figure 9 *Bronze coins from cargo f.*

The hammering of the surface has compacted the volume directly underneath and its effect has decreased progressively up to the mass heart. The surface opposite the hammered surface shows little compaction, as if the hammering had taken place on a soft surface, not causing important repercussions. The crude mass is extremely fragile and may break during the first treatment under excessive hammering (Fluzin and Leclere 1998; Fluzin 2002). Seemingly, for this partly consolidated bloom, hammering took place on soft ground. Tracing lines formed by successive compactions demonstrate this scenario (Fig. 10).

Short pointed bar A047 This is a small bar of a rectangular section, elongated with blunt ends, which is 39 cm long and weighs 3 kg (Fig. 13). Its maximum thickness is slightly off-centre, separating the bar into two unequal portions of 19 and 20 cm. Its maximum cross-section is 5×3.5 cm. Two surfaces of the quadrangular section are relatively flat. The other two are irregular, having a slight concavity. The edges and both ends are blunt, perhaps due to a corrosion of the periphery. The section—cut at the maximum thickness of the semi-products—is slightly heterogeneous. Some areas, consisting of metal interspersed by numerous inclusions, are adjacent to 'cleaner', homogeneous areas. Overall, the metal shows relatively good inclusions cleaning, with an impurity rate of 8.9% of the cut surface.[5] Metallographic analysis reveals a considerable heterogeneity of the metal mass. Numerous inclusions have remained: their

[5]See also Supplementary item 8.

14754754, 2015, 3, Downloaded from https://onlinelibrary.wiley.com/doi/10.1111/arcm.12077 by Hanshin University, Wiley Online Library on [31/03/2026]. See the Terms and Conditions (https://onlinelibrary.wiley.com/terms-and-conditions) on Wiley Online Library for rules of use; OA articles are governed by the applicable Creative Commons License

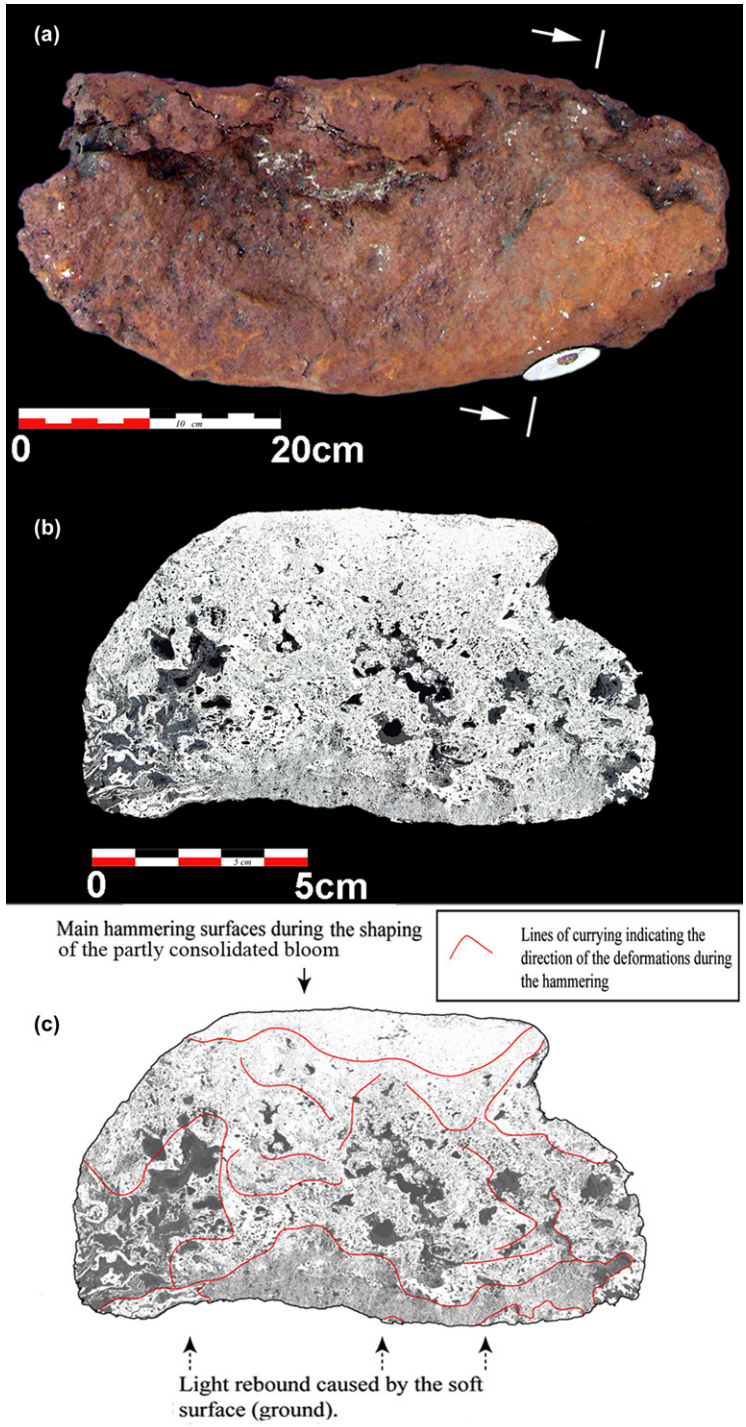

Figure 10 *Partly consolidated bloom A108: (a) the top surface—the white lines indicate the position of the cutting; (b) a cross-section; (c) deformations created during shaping.*

14754754, 2015, 3, Downloaded from https://onlinelibrary.wiley.com/doi/10.1111/arcm.12077 by Hanshin University, Wiley Online Library on [31/03/2026]. See the Terms and Conditions (https://onlinelibrary.wiley.com/terms-and-conditions) on Wiley Online Library for rules of use; OA articles are governed by the applicable Creative Commons License

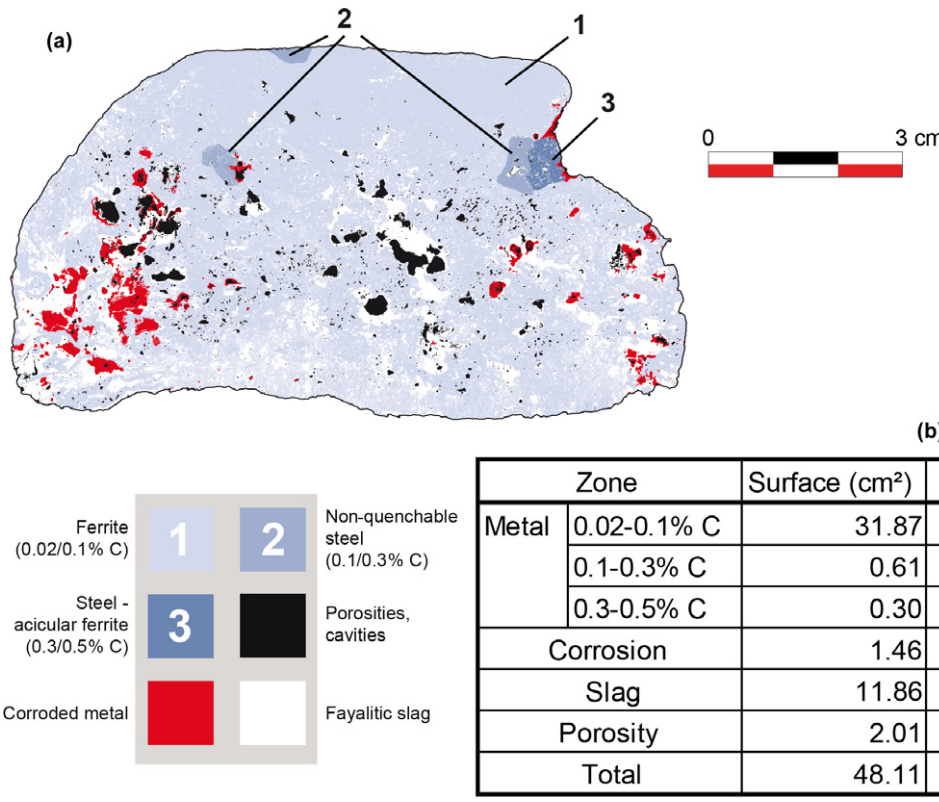

Zone		Surface (cm²)	%
Metal	0.02-0.1% C	31.87	66.25
	0.1-0.3% C	0.61	1.26
	0.3-0.5% C	0.30	0.63
Corrosion		1.46	3.03
Slag		11.86	24.65
Porosity		2.01	4.18
Total		48.11	100.00

Figure 11 *Image analysis of the section of partly consolidated bloom A108: (a) a cross-section; (b) elements.*

morphologies represent the whole gamut, from inclusions having rounded edges, mainly located in the centre of the object (Fig. 14, 001/002/003/004), to flattened and elongated inclusions in the periphery (Fig. 14, 005/006/007). The metal-to-slag proportion is heterogeneous: slag inclusions in the metal and sometimes beads and strings of metal in the slag (Fig. 14, 008/009/010). These structures represent the preservation of the structure of a heterogeneous metal crude mass in which the periphery was hammered. Most slag is composed of iron silicate of fayalite type, with dendrite and globules of wüstite. Most sections consist of irregular ferrite grains (0.02% C) with rather rounded joints (97.6% of the metal surface) (Fig. 14, 011/012). Very locally, at the periphery, a higher carburization is detectable, up to concentrations of 0.5–0.6% C, in the form of acicular ferrite (Fig. 14, 013). In other peripheral parts, the carbon content is lower (Fig. 14, 014/015/016). The inclusions have an irregular and jagged morphology, with stretching and squashing related to the direction of hammering (currying lines) (Fig. 13, c). The lines formed by the squashing underline the preferential hammering surfaces and the work intensity on each side. Obviously, two of the surfaces were more intensely hammered than the others (Fig. 13, c). These two faces are adjacent, and according to the curvature of the currying lines, the initial mass could have been approximately round. This shape, forming flat surfaces, implies that the centres of the hammered faces are more distorted than their peripheries. A pinching is also visible at the junction between the hammered sides. The deformations of the other two sides, caused by anvil repercussions (or some other hard passive surface), are less distorted. This occurs when a

14754754, 2015, 3, Downloaded from https://onlinelibrary.wiley.com/doi/10.1111/arcm.12077 by Hanshin University, Wiley Online Library on [31/03/2026]. See the Terms and Conditions (https://onlinelibrary.wiley.com/terms-and-conditions) on Wiley Online Library for rules of use; OA articles are governed by the applicable Creative Commons License

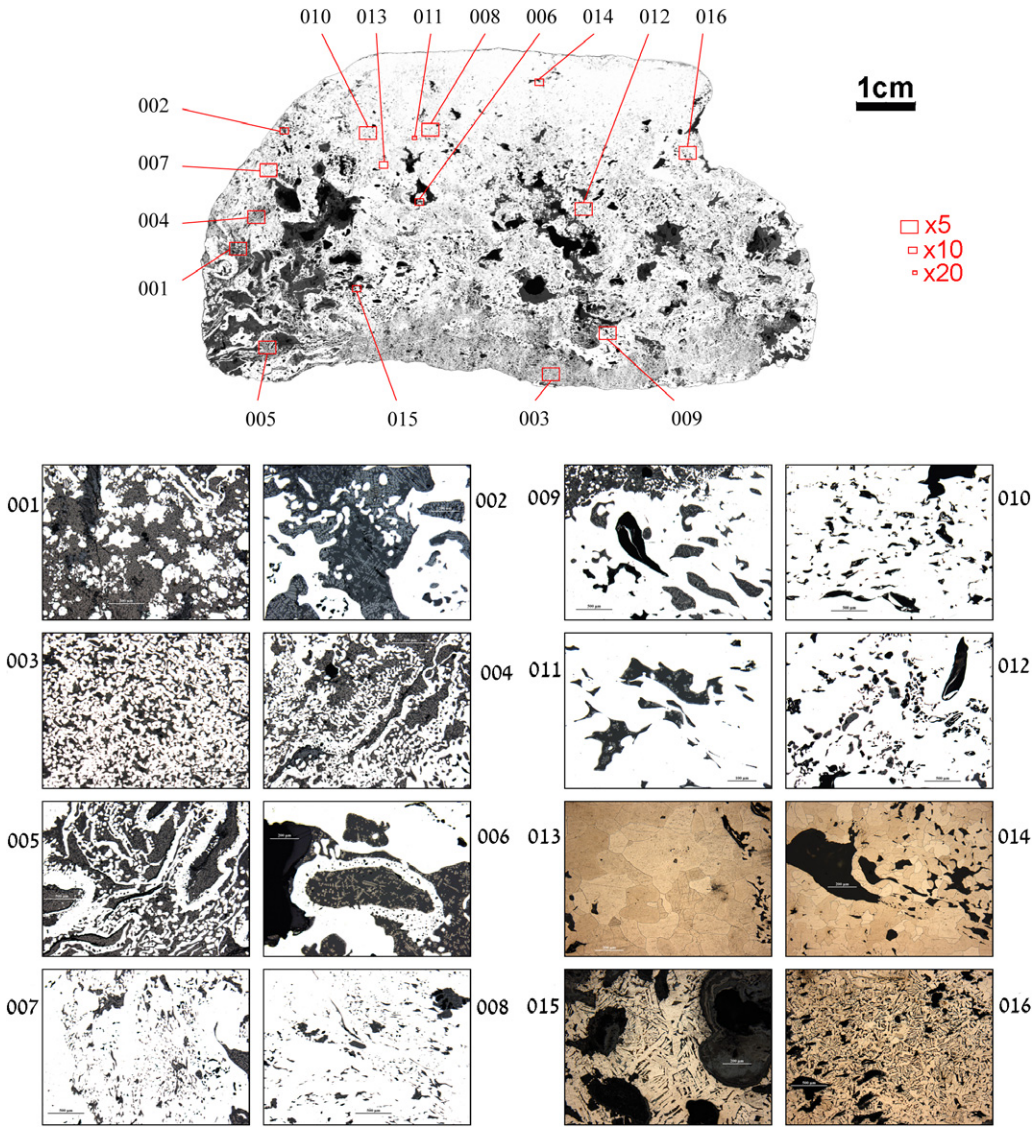

Figure 12 *The metallographic study of partly consolidated bloom A108.*

quadrangular section is desired. The blacksmith hammers one side of the piece, then rotates it a quarter turn (90°), hitting the adjacent face, returns to the first side and so on. Both sides are well hammered; the others are deformed by the anvil repercussion.[6]

Elongated pointed bar A004 This is a square-section metal bar (2.6–2.7 cm maximum thickness) with elongated and blunt ends (Fig. 15): it is 34 cm long and weighs 950 g. Its morphology does not show any broken curve at its maximum thickness. The four sides are consequently

[6]Supplementary item 7.

14754754, 2015, 3, Downloaded from https://onlinelibrary.wiley.com/doi/10.1111/arcm.12077 by Hanshin University, Wiley Online Library on [31/03/2026]. See the Terms and Conditions (https://onlinelibrary.wiley.com/terms-and-conditions) on Wiley Online Library for rules of use; OA articles are governed by the applicable Creative Commons License

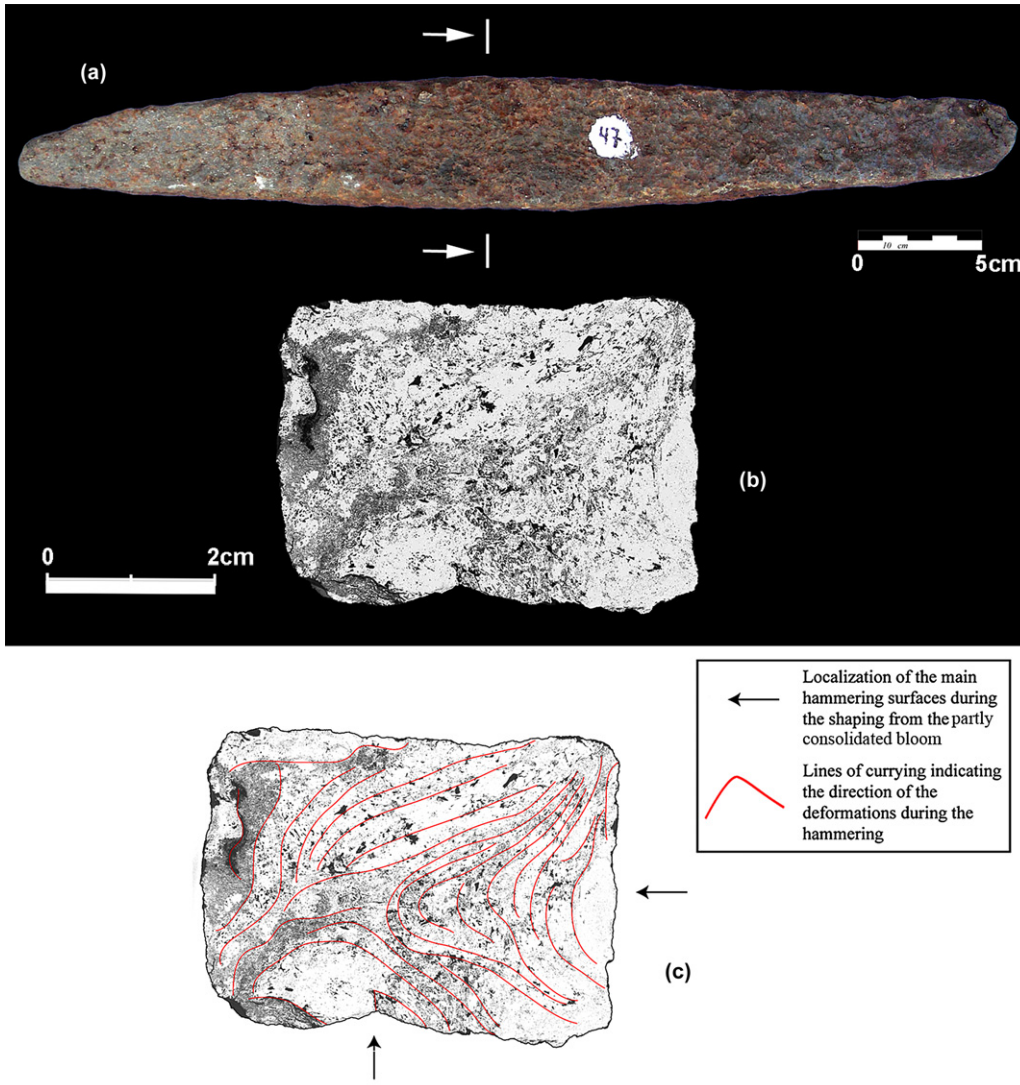

Figure 13 *Short pointed bar A047: (a) the top surface—the white lines indicate the position of the cutting; (b) a cross-section; (c) deformations caused during shaping.*

slightly curved and regular. The section—cut at its maximum thickness—shows relatively dense and compacted metal. Some large slag inclusions have remained on two thirds of the surface, the final third consisting of areas composed of numerous thinner inclusions. Two small cracks are visible along one edge. The proportion of impurities in the section is 9.8%.[7] Studying the section using a metallographic microscope reveals numerous slag inclusions. They consist of iron silicates of fayalite type, loaded by globules and dendrites of wüstite (Fig. 16, micro 001–010). Where the inclusions are larger, they have a jagged morphology and a deformation (flattening)

[7]See also Supplementary item 9.

14754754, 2015, 3, Downloaded from https://onlinelibrary.wiley.com/doi/10.1111/arcm.12077 by Hanshin University, Wiley Online Library on [31/03/2026]. See the Terms and Conditions (https://onlinelibrary.wiley.com/terms-and-conditions) on Wiley Online Library for rules of use; OA articles are governed by the applicable Creative Commons License

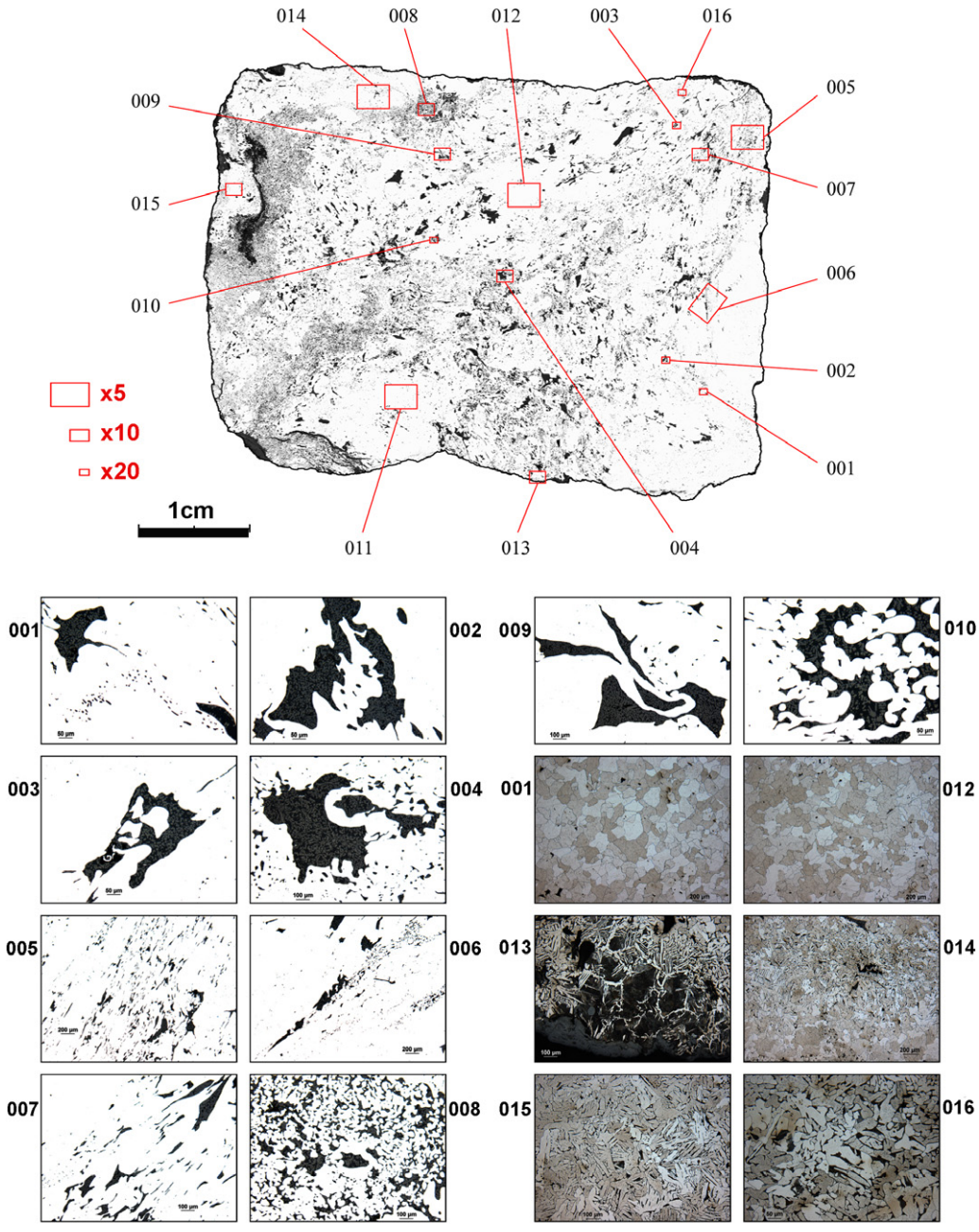

Figure 14 *The metallographic study of short pointed bar A047.*

caused by hammering, which indicates the preferred direction of plastic deformation (Fig. 16, 002/003/004/007/008). In areas with thinner, numerous inclusions, the general morphology is also jagged, but the distortion is less visible (Fig. 16, micro 005). When inclusions are adjacent to the periphery, corrosion was facilitated by the presence of non-metallic elements (Fig. 16,

14754754, 2015, 3, Downloaded from https://onlinelibrary.wiley.com/doi/10.1111/arcm.12077 by Hanshin University, Wiley Online Library on [31/03/2026]. See the Terms and Conditions (https://onlinelibrary.wiley.com/terms-and-conditions) on Wiley Online Library for rules of use; OA articles are governed by the applicable Creative Commons License

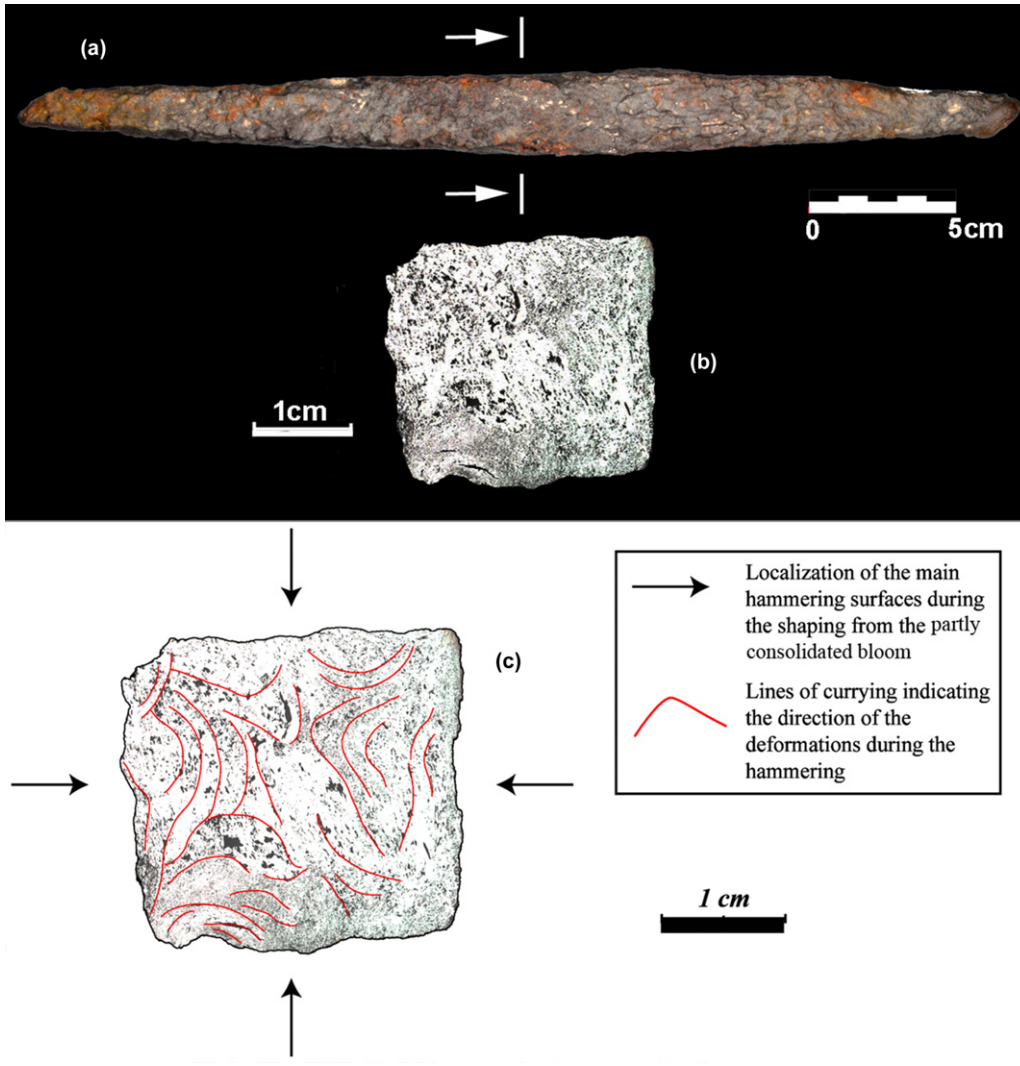

Figure 15 *Elongated pointed bar A004: (a) the top surface—the white lines indicate the position of the cutting; (b) a cross-section; (c) deformations during shaping.*

micro 001). The structures examined did not show an ore initial structure. Nital etching shows an iron/carbon composition of over 98% of equiaxed ferrite (0.02% C) (Fig. 16, micro 011). Only two very small areas were more carburized locally, up to 0.6–0.7% C (Fig. 16, 012/013/014/015). Inclusion lines and crushings related to deformation facilitate a deciphering of the bar's 'history' (Fig. 15 (c)). All four sides seem to have been hammered. However, two contiguous sides have a different texture from the others, with a greater number of very small inclusions. The other two show a denser texture, but the inclusions are much larger. Possibly initially, two adjacent faces were hammered as shown above (short pointed bar A047) and, in a second step, the other two were then finished.

14754754, 2015, 3, Downloaded from https://onlinelibrary.wiley.com/doi/10.1111/arcm.12077 by Hanshin University, Wiley Online Library on [31/03/2026]. See the Terms and Conditions (https://onlinelibrary.wiley.com/terms-and-conditions) on Wiley Online Library for rules of use; OA articles are governed by the applicable Creative Commons License

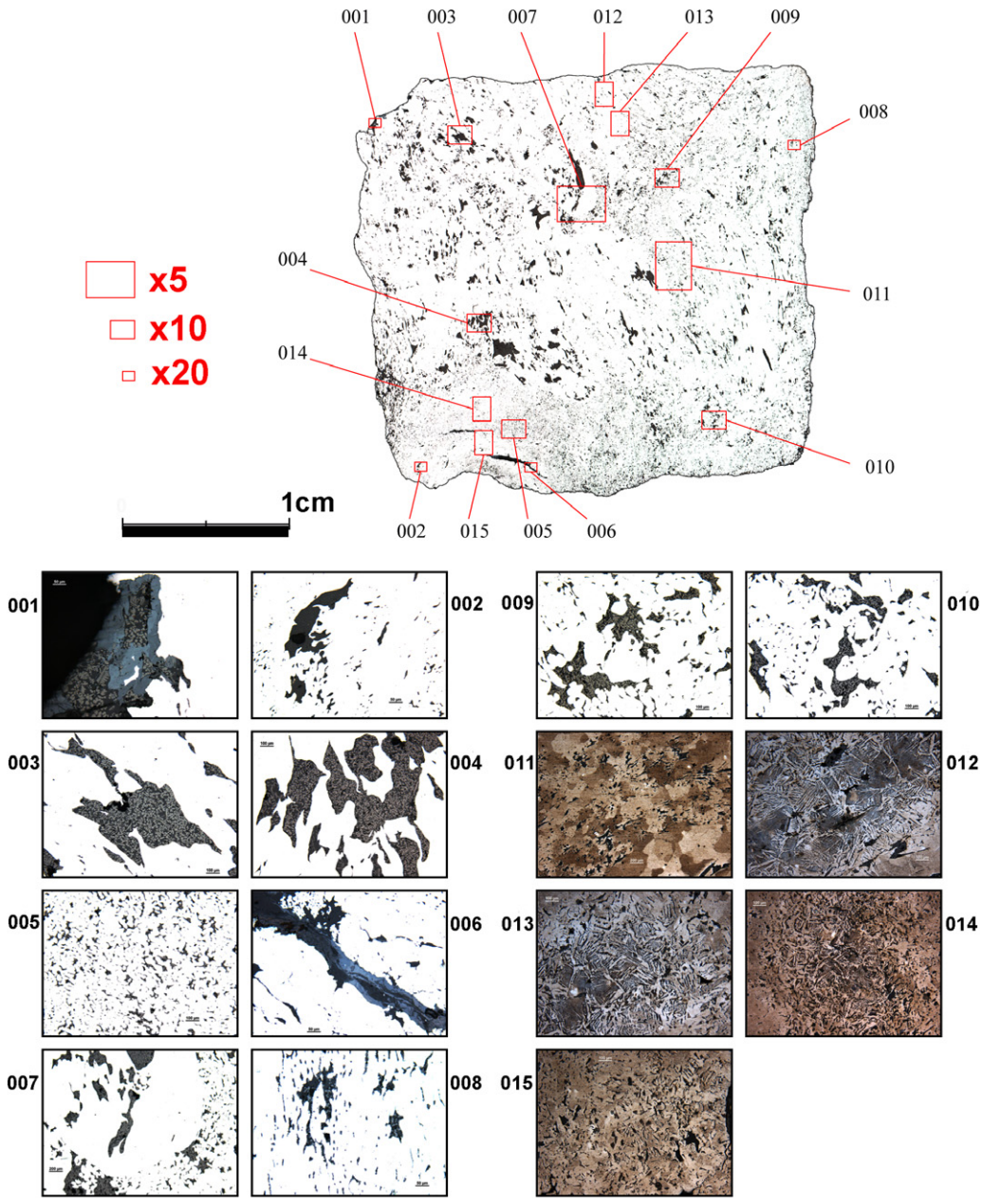

Figure 16 *The metallographic study of elongated pointed bar A004.*

Major elemental composition of slag inclusions by SEM coupled with an EDS analyser

Partly consolidated bloom A108 Chemical analysis of major elements was performed on 445 inclusions from 11 different zones on the cross-section.[8] First, in terms of mass% P_2O_5** and

[8]Supplementary item 6a.

14754754, 2015, 3, Downloaded from https://onlinelibrary.wiley.com/doi/10.1111/arcm.12077 by Hanshin University, Wiley Online Library on [31/03/2026]. See the Terms and Conditions (https://onlinelibrary.wiley.com/terms-and-conditions) on Wiley Online Library for rules of use; OA articles are governed by the applicable Creative Commons License

mass% MnO**, their content is much reduced or even non-existent. The ratios mass% Al_2O_3/mass% SiO_2 and mass% CaO/mass% SiO_2 are relatively constant.[9] However, the ratios mass% K_2O/mass% CaO and mass% MgO/mass% Al_2O_3 have a higher dispersion.[10] This dispersion is mainly due to the low amounts of K_2O and MgO, mostly less than 0.5 mass%. Because of the detection limit of the EDS analyser, values below 0.5 mass% have an error margin of 100% and blur the clarity of the results. A major elements analysis of mass A108 therefore indicates a much reduced amount of specific markers other than mass% CaO and mass% SiO_2.

Short pointed bar A047 In the bipyramidal semi-product A047, 11 elementary maps with 164 inclusions were analysed.[11] Similarly to mass A108, in semi-product A047, the element values mass% P_2O_5** and mass% MnO** are very low, indicating that the reduction did not use materials that were rich in phosphorus or manganese. The ratios mass% Al_2O_3/mass% SiO_2 and mass% CaO/mass% SiO_2 are, as for the other metal mass, markedly constant.[12] The ratios mass% K_2O/mass% CaO and mass% MgO/mass% Al_2O_3 are more scattered for the same reasons.[13] The concentrations of mass% K_2O and mass% MgO are slightly higher than for A108, and thus it is possible to see more clearly a lower dispersion of values than in cases of 0.5 mass%.

Elongated pointed bar A004 Nine elementary mappings were performed on the elongated bar A004.[14] The major elements compositions of 279 inclusions were measured. In that semi-product, elements P_2O_5 and MnO also have very low mass%** values. This means that these elements are not characteristic of the reduction system involved in manufacturing this semi-product. The ratios mass% Al_2O_3/mass% SiO_2 and mass% CaO/mass% SiO_2 are markedly constant, while the ratios mass% K_2O/mass% CaO and mass% MgO/mass% Al_2O_3 show a greater dispersion.[15] Here, it is the ratio mass% MgO/mass% Al_2O_3 that is most lacking, since the MgO content is less than 0.5 mass%.

The major elements compositions of the three semi-products reveal a quite similar comportment, with a very low proportion of P_2O_5, MnO, MgO and K_2O and a high CaO content. We will compare these results further below (cf., 'Typology and composition of cargo a').

DISCUSSION

Formation of sites

Over millennia, ships sailing along the Israeli coast were driven ashore by storms and wrecked (Galili *et al*. 2002) (Fig. 1). The discussed shipwrecks probably occurred while sailing or anchoring along the Carmel coast. Recent human interference with the coast has resulted in erosion and exposure of wreck sites, where usually only heavy objects have remained. Thus the wrecked ships probably contained materials that have been lost. The Dor assemblage probably represents a watercraft that was wrecked while mooring in the semi-sheltered south anchorage.

[9]Supplementary items 6b and 6e, respectively.
[10]Supplementary items 6c and 6d, respectively.
[11]Supplementary item 10a.
[12]Supplementary items 10b and 10e, respectively.
[13]Supplementary items 10c and 10d, respectively.
[14]Supplementary item 11a.
[15]Supplementary items 11b, 11c and 11d, respectively.

14754754, 2015, 3, Downloaded from https://onlinelibrary.wiley.com/doi/10.1111/arcm.12077 by Hanshin University, Wiley Online Library on [31/03/2026]. See the Terms and Conditions (https://onlinelibrary.wiley.com/terms-and-conditions) on Wiley Online Library for rules of use; OA articles are governed by the applicable Creative Commons License

Typology and composition of cargo a

Several parameters influence the type and quality of semi-products: (1) the quality of the initial partly consolidated blooms influences compaction and size; (2) the proficiency of the craftsman affects compaction and material loss during refining; (3) the semi-product end use affects its final shape—an elongated, well-compacted, bar is suitable for manufacturing small artefacts, while an anvil or an anchor requires large partly consolidated blooms; (4) the technocultural context dictates the morphology, which may symbolize quality; and (5) marketing affects the character of the product. In iron and steel production, refining is one of the most difficult stages of the *chaîne opératoire*. During this phase, more than half of the weight of the initial partly consolidated bloom is lost. Clearly, the final costs of an initial partly consolidated bloom and an elongated bar differ greatly. Consequently, and according to the archaeological discoveries, semi-products may take the form of roughly refined partly consolidated blooms, bars, folded-over leaves, salmon shapes, bipyramids, blanks, currency bars or socket bars (Bauvais and Fluzin 2009; Berranger and Fluzin 2012). The quality of the refining work may also be evaluated from the viewpoint of concomitant characteristics: the level of impurities (porosity and inclusion rate); the morphology of the porosities and inclusions (deformation); and the number and morphology of folds and the homogeneity of the iron/steel. The metallographic analysis of the three semi-products reveals that they correspond to at least two, or even three, metal compaction stages after exiting the shaft furnace. The first stage is represented by semi-product A108. That semi-product results from a preliminary compaction of an initial bloom that, by definition, is fragile and little compacted. It requires a first hammering to densify it and to manipulate it further without risking fragmentation (particularly during transport). Consequently, the first hammering had to be 'soft', in order not to weaken the iron, which is why A108 was manipulated on a soft surface (soil, wooden block). Both bars representing further treatment demonstrate advanced stages of metal compaction. In spite of a high proportion of impurities (8.9% and 9.8%), the metal is well compacted and can undergo a deformation without risking breakage. Short pointed bar A047 seems to have been hammered only on two of its adjacent sides, the others having undergone only anvil repercussion, while elongated pointed bar A004 has been hammered on its four sides. These differences are related to their morphology: one, hammered on two sides, has a rectangular cross-section, while the other has a square section and was hammered on all four. The smaller section of A004 and its lower weight may also indicate a more advanced compaction, although, as discussed later, there is no evidence that clearly links A047 and A004 to a pre-designed technical succession. From the viewpoint of the iron/carbon composition, the three semi-products are identical. They lack phosphorus and their carbon content is very low (mostly ferritic iron). Seemingly, their composition is unrelated to morphological differences. However, when their weights are considered, bars A004 and A047 certainly cannot be a direct result of the compaction of a partly consolidated bloom, as in the case of A108. Semi-product A108 weighs 7.1 kg (the average of the other partly consolidated blooms of cargo a is 10.2 kg) while the bars A004 and A047 weigh 0.950 and 3 kg, respectively. Numerous forging experiments conducted during treatments of partly consolidated blooms demonstrate a considerable material loss during compaction (fallen slag, pieces of metal etc.). The proportion of loss decreases as the thermomechanical treatment is performed (Crew 1991; Crew and Crew 1994; Dillmann *et al*. 1997; Leroy *et al*. 2012). The loss between the initial bloom and partly consolidated bloom stages is about 50% of the starting mass. It is possible to estimate the weight of the partly consolidated bloom from which A108 (7.1 kg) was derived at about 14 kg. During the next step, to form a short and stocky bar

14754754, 2015, 3, Downloaded from https://onlinelibrary.wiley.com/doi/10.1111/arcm.12077 by Hanshin University, Wiley Online Library on [31/03/2026]. See the Terms and Conditions (https://onlinelibrary.wiley.com/terms-and-conditions) on Wiley Online Library for rules of use; OA articles are governed by the applicable Creative Commons License

(corresponding to a short pointed bar semi-product), the estimated losses are 30% of the partly consolidated bloom. Semi-product A047, weighing 3 kg (the average of the other short pointed bars is 2.23 kg), would be derived from a partly consolidated bloom weighing about 4 kg. Semi-product A004, weighing 0.950 kg (the average of the other elongated pointed bars is 1.9 kg), corresponds to the third stage of compaction, and the losses can be estimated at around 20%. Thus, this bar would have been derived from a pre-compacted bar weighing about 1.2 kg.

Clearly, each of the three studied semi-products did not originate directly in the semi-product representing the previous technical stage. Either these semi-products did not originate from the same *chaîne opératoire*, or an additional cutting step was executed. If one compares the chemical analysis results of each semi-product on a bivariate graph (mass%* and mass%**), it is evident that the three semi-products have slight variations. It is only by integrating data from other sets of analysed samples that their resemblance is particularly underlined (Fig. 17). The four graphs in Figure 17 include the results obtained for the three samples discussed here. To better represent their possible variation, the results obtained for two additional sets of data have been added: a set of bipyramidal semi-products from eastern France, dating from the local early Iron Age (800–500 BC) and a set of semi-products formed as quadrangular bars, coming from Roman-period shipwrecks found off Saintes-Maries-de-la-Mer (Pagès *et al*. 2008, 2011). The three semi-products have a strong resemblance, a very low content of discriminating elements (P_2O_5, MnO, MgO and K_2O) and a high CaO content. Discriminating by the content of one or more elements present in high concentration appears to be credible and defensible; a characterization by an absence is of less value. However, the present case is based on the analysis of seven elements and the picture as a whole (both the absence and the strong presence) can validate such discrimination.

The interpretation based on these preliminary results may indicate that the three semi-products (the reduction technology of which used materials with very low contents of K_2O, MgO, MnO and P_2O_5 and rich in CaO content) originated in very similar, perhaps identical, manufacturing systems. Further analysis of the trace elements by ICP–MS is necessary to assure such a common origin.

Commercial and technological observations on cargo a

The analyses of the three types of semi-products present in cargo a enables us to draw some conclusions regarding the commercial/technological function of that cargo and the intended market. First, assuming that these three types of semi-product came from one or more workshops in a small geographical and technocultural area, it is noteworthy that their morphology is not an indication of the metal origin. The fact that all three have an identical iron/carbon composition also indicates that their shapes were not intended to mark an alloy type. Finally, the degree of compaction of the three semi-products, the partly consolidated bloom and the two bars (the short pointed bar and the elongated pointed bar) differs. It is simple to differentiate between these two groups on the basis of compaction quality. However, the degrees of compaction of the short pointed bar and the elongated pointed bar are close, but their morphologies vary: short pointed bars are massive and stocky, while elongated pointed bars contain less material. These differences may reflect a treatment related to their intended final use. To summarize, we have analysed and discussed three types of semi-products, probably from the same origin, distinguished by their shapes and the amount of material they contain. One stands out from the others by its low degree of compaction and the other two are distin-

14754754, 2015, 3, Downloaded from https://onlinelibrary.wiley.com/doi/10.1111/arcm.12077 by Hanshin University, Wiley Online Library on [31/03/2026]. See the Terms and Conditions (https://onlinelibrary.wiley.com/terms-and-conditions) on Wiley Online Library for rules of use; OA articles are governed by the applicable Creative Commons License

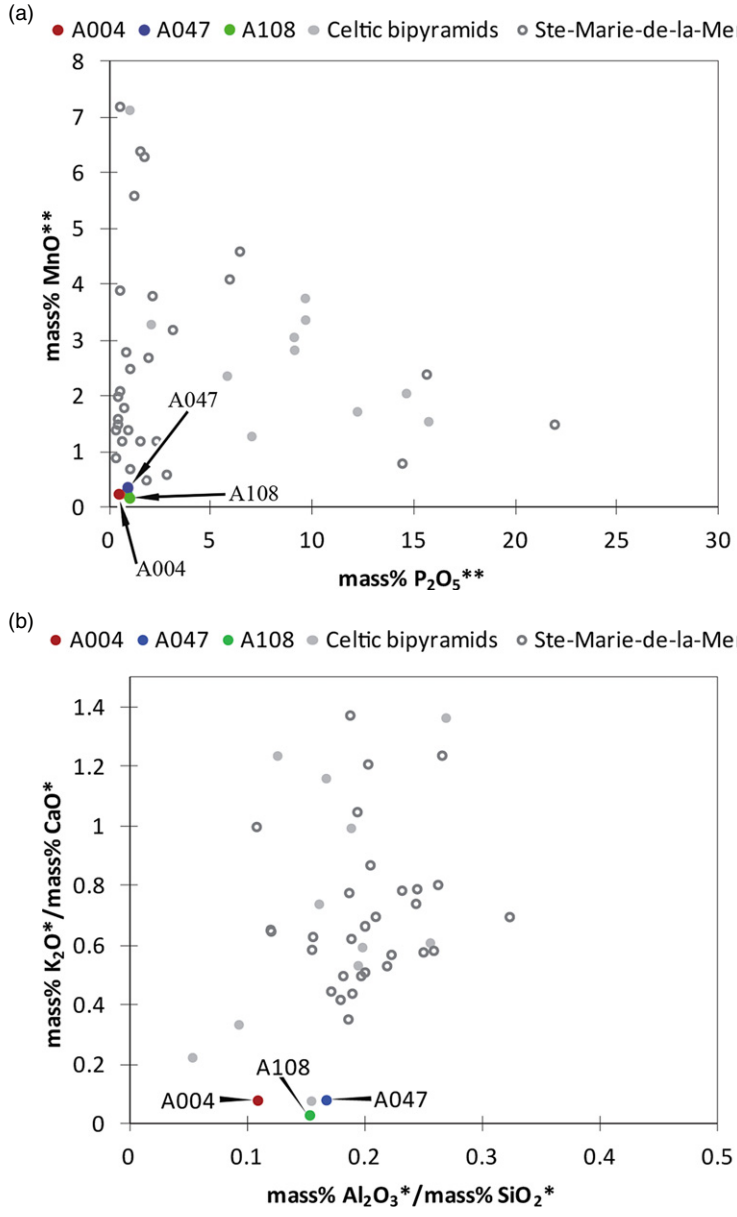

Figure 17 *Values of Israeli semi-products and values of unpublished bipyramidal semi-products from eastern France (grey dots), with bars from Saintes-Maries-de-la-Mer (Pagès* et al. *2008) (grey circles) for comparison. (a) P_2O_5** and MnO** contents measured in SI; (b) NRC ratios in SI—Al_2O_3*/SiO_2* versus K_2O*/CaO*; (c) NRC ratios in SI—MgO*/Al_2O_3* versus CaO*/SiO_2*; (d) NRC ratios in SI–MgO*/Al_2O_3* versus K_2O/CaO*.*

guished by their morphology. These considerations imply that the market for which the cargo was intended was complex enough to demand three semi-product forms. Moreover, the blacksmiths–artisans in that intended market were highly proficient. They were able to further transform an almost raw iron mass, a very complex technique. Furthermore, the essentially

14754754, 2015, 3, Downloaded from https://onlinelibrary.wiley.com/doi/10.1111/arcm.12077 by Hanshin University, Wiley Online Library on [31/03/2026]. See the Terms and Conditions (https://onlinelibrary.wiley.com/terms-and-conditions) on Wiley Online Library for rules of use; OA articles are governed by the applicable Creative Commons License

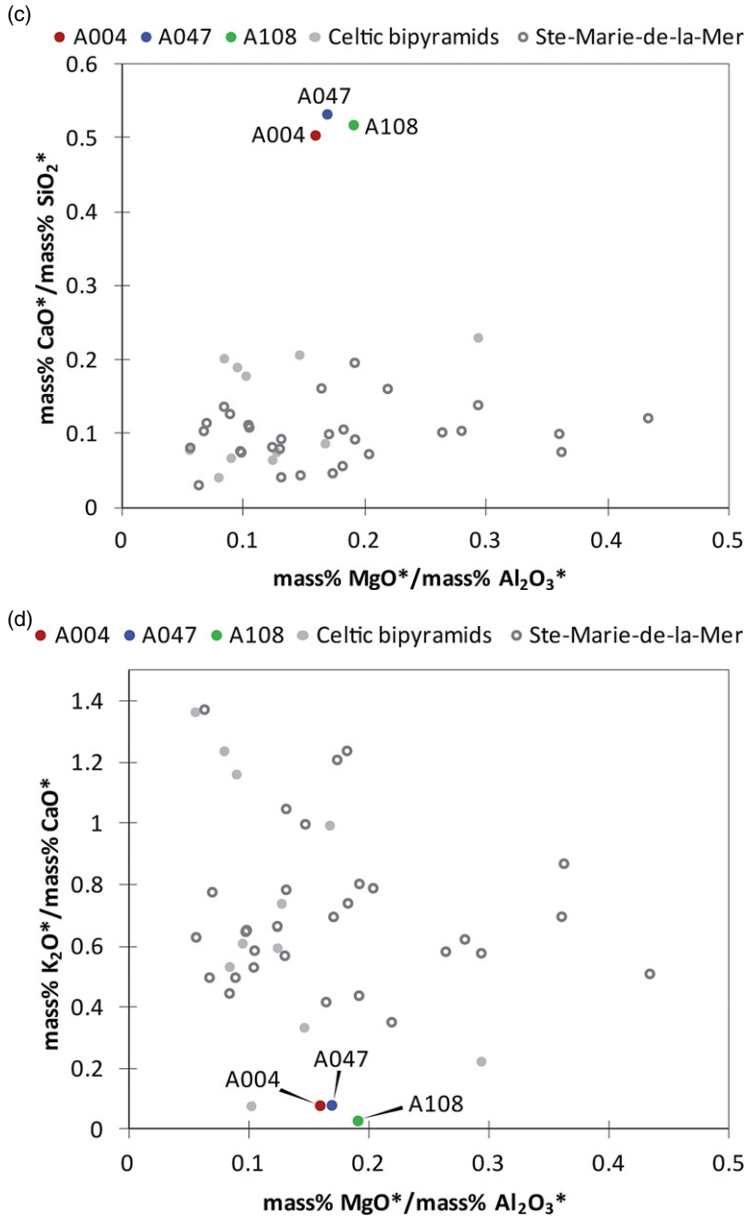

Figure 17 *(Continued)*

ferritic composition of the semi-products involves mastery of the case-hardening technique, aiming at producing a more carburized metal, steel. This technique is among the most complex in iron production (Bauvais and Fluzin 2009). These activities were highly specialized, as they demanded the presence of two types of pre-treated materials, with striking but relatively minute functional differences.

14754754, 2015, 3, Downloaded from https://onlinelibrary.wiley.com/doi/10.1111/arcm.12077 by Hanshin University, Wiley Online Library on [31/03/2026]. See the Terms and Conditions (https://onlinelibrary.wiley.com/terms-and-conditions) on Wiley Online Library for rules of use; OA articles are governed by the applicable Creative Commons License

Iron production in the South Levant

Societies engaging in agriculture, manufacturing, stone and timber construction and shipbuilding need iron. Military activities increase such demands. The importance of the iron supply to such cultures is obvious. The main limitations on the iron- and steel-making industry, from the ore to the working tool, are geological and environmental. In the territory from Tripoli in Lebanon, to the Negev in modern Israel, and from Amman in the east to the Mediterranean, regional ore deposits have always been poor. Limited amounts of iron oxide were available in the Rift Valley region (Einecke 1950; Rohrlich *et al*. 1980). The historical populations of the Israeli coast had no access to substantial iron ore sources. Since the start of the Iron Age, much of the iron needed for the ongoing civil and military activities must have been imported. Political agreements and commercial alliances were necessary to provide it (Bauvais 2008). A famous Old Testament episode, 1 Samuel 13:19–22, illustrates a similar situation. Iron production in Jordan, a part of the Levant, was recently reviewed (Bani-Hani *et al*. 2012). Direct or 'bloomer' was the main method used for smelting of iron ores, followed by smithing. This, most probably, was the state of technology from the Bronze Age to the Umayyad Period (seventh to eighth centuries AD) and perhaps later (Bani-Hani *et al*. 2012).

The demand for iron in the Levant during the Byzantine and medieval periods

Historical data on Levantine iron trading and manufacturing relevant to the present study—that is, during the Byzantine and early medieval periods—indicate a constant civilian and military demand for iron. Such a demand must have continued during the Early Islamic period. Later, during the intensive wars characterizing the Crusader period, iron was greatly in demand. Acts of war, movements of armies, stone quarrying and fortress building were intense and demanded much imported iron. The need for ship's stores (anchors, chains, tackle, rigging) and harbours (port-protecting chains, gates, fortifications, bollards) increased such demands. The home countries of the Crusaders were very remote and the armies must have produced and maintained their own weapons, tools and vehicles. Therefore, during the Crusader period, the demand for iron was probably higher than in the previous, Roman, Byzantine and Early Islamic periods. Most probably, large quantities of iron were imported to the Crusader lands together with craftsmen and means of production. The production and maintenance of numerous iron artefacts explain the presence of artisans associated with forging. For example, a forge with its tools was discovered in the Crusader castle of Mezad Ateret (*Vadum Iacob*) in the northern Jordan Valley. The building of the castle lasted for 11 months. About 20 000 blocks of hard stone were quarried, cut, transported and placed in that short period (Ellenblum 2001). Such intense building activity, in addition to producing and maintaining arms—for example, disposable arrowheads, armour and hand weapons—consumed much iron. In the Crusader fortress of Atlit, a thick layer of ashes containing numerous forging slag cakes were recovered (Ronen and Olami 1978, fig. 2, area 26). A few metres west of this area, two round ovens were found: one (4 m in diameter) was constructed of burnt mud bricks and the other (5 m in diameter) was built of stones. Amounts of smithing slag were found in and around these installations (Ronen and Olami 1978, 41, 44, 45). Thus these ovens could also have been used in forging.

The origin and the organization of the transportation of semi-products

Land transportation of heavy cargoes is not economically viable. Iron imports by land were expensive, rare or totally absent. Probably since Roman times—that is, the first century AD—iron

14754754, 2015, 3, Downloaded from https://onlinelibrary.wiley.com/doi/10.1111/arcm.12077 by Hanshin University, Wiley Online Library on [31/03/2026]. See the Terms and Conditions (https://onlinelibrary.wiley.com/terms-and-conditions) on Wiley Online Library for rules of use; OA articles are governed by the applicable Creative Commons License

was generally imported by sea as semi-products or final products (Bauvais 2008). During the Levantine Byzantine period, most armies were supplied from relatively close imperial centres in Constantinople and Southern Europe. The Islamic conquests of the mid-seventh century upset these networks, but new ones were probably reconstructed. The Crusades (12th–13th centuries), generated an iron trade with European entities. Christian states simultaneously tried to restrict iron trade with the Muslims because iron (and timber) were strategic war materials (i.e., chains: Bauvais 2008; Kedar 2012). The Crusader coins (cargo a) were minted in the Latin Kingdom of Jerusalem, to where the iron cargo was heading. Coins are used to date shipwrecks, but they also yield information on the ship's last voyage and origin, as people leaving a country may exchange money into the coinage of port of destination. It is also conceivable that the iron-carrying ship was trading between coastal ports in the Crusader kingdom. The sliced gold coins may indicate such activity.

In the Third Lateran Council of 1179, Pope Alexander III forbade the trade of war materials with the Muslim countries (Jacoby 2001; Stantchev 2009). The ban was often renewed during the 13th and 14th centuries; obviously, it was hard to enforce this ban. Ashtor (1986, 1983) showed that the profit of iron traders was about 300%, causing this trade to become secret and undocumented. In the 14th century, two trade routes were followed by Venetians supplying this illicit market. One passed through Crete, Constantinople and Tana. The other went to Crete, Aïas and Akko (Acre) (Sprandel 1970). After the establishment of the Ottoman Empire (early in the 16th century), the iron trade became partly documented. But knowledge about it is incomplete, because it was often illegal and unregistered. Documents from the 15th century show that Bursa was an iron production centre, exporting to Egypt and Syria (Inalcik 1960). Maritime trade increased after the Ottoman conquest of Rhodes and Cyprus in the 16th century; however, no text refers to direct trade with what is now the Israeli coast. The main commercial hubs were Aleppo and Alexandria. Redford (2012) reported on a 12th–13th century production centre of iron in Kinet, on the south coast of Anatolia. It produced iron blooms which may have been exported to Egypt. Jaffa and Acre are not mentioned as trade destinations from Bursa (Bauvais 2008) or from other trading centres. Due to the scarcity of documentation, the iron cargoes discussed here fill an important lacuna in the technological–commercial history of the South Levant.

CONCLUSIONS

Semi-products in sunken cargoes, discovered off the Carmel coast, represent a trade lasting for about a millennium.

The semi-products from cargoes b, d and f, dated to the Byzantine period, were intended for military and civil purposes. They could have been imported from Anatolia or Venice. Further investigations are needed to ascertain their modes of manufacture and their origin.

The semi-products from cargo a, dated to about 1130–1200 CE, could have originated in Christian Europe and been shipped to Frankish military and civilian markets in the Levant. Alternatively, they could represent 'contraband'—forbidden trade between Italian republics and Muslims. As far as we know, this is the first concrete evidence of that widely documented material.

Cargoes e and c, dated to between the 15th and the 19th centuries, represent contemporary Levantine iron trade. The iron would have originated in an Ottoman or a European port. However, no documentation of South Levantine ports as destinations for the metal trade is known.

All the Carmel coast shipwrecks studied carried partly consolidated blooms (billets). This product, which is rare in long-distance trade, so far has no known parallels in Levantine

14754754, 2015, 3, Downloaded from https://onlinelibrary.wiley.com/doi/10.1111/arcm.12077 by Hanshin University, Wiley Online Library on [31/03/2026]. See the Terms and Conditions (https://onlinelibrary.wiley.com/terms-and-conditions) on Wiley Online Library for rules of use; OA articles are governed by the applicable Creative Commons License

shipwreck cargoes or Levant coast production centres. Thus such semi-products could characterize an overseas production region that is as yet unidentified.

A further study of the iron cargoes recovered off the Carmel coast is necessary to present a better picture of Levantine iron manufacturing and trade.

The study of trace elements in semi-products from the Camel coast may help to link them to a regional signature.

ACKNOWLEDGEMENTS

The research was funded by the Israel Antiquities Authority and the University of Haifa. We thank S. Ben-Yehuda for the drawing of Figure 6 and Supplementary item 5, J. Galili for the photographs, and S. Arenson, D. Jacoby and D. Syon for their comments.

REFERENCES

Ashtor, E., 1983, *Levant trade in the later Middle Ages*, Princeton University Press, Princeton, NJ.

Ashtor, E., 1986, *East–West trade in the medieval Mediterranean*, Variorum Press, London.

Bani-Hani, M., Abd-Allah, R., and El-Khouri, L., 2012, Archaeometallurgical finds from Barsinia, northern Jordan: microstructural characterization and conservation treatment, *Journal of Cultural Heitage*, **13**, 314–25.

Bauvais, S., 2007, *Evolution de l'organisation des activités de post-réduction dans le Nord du Bassin Parisien au 2nd Age du fer: études multidisciplinaires de la chaîne opératoire en métallurgie du fer*, Ph.D. dissertation, Université de Technologie de Belfort Montbéliard, Belfort/Université de Besançon, Besançon.

Bauvais, S., 2008, Prolégomènes à une histoire de la métallurgie du fer au Levant Sud, *Bulletin du Centre de Recherche Français de Jérusalem*, **19**.

Bauvais, S., and Fluzin, P., 2009, Archaeological and archeometrical approaches of the *chaîne opératoire* in iron and steelmaking: methodology for a regional evolution study, in *Techniques and people: anthropological perspectives on technology in the archaeology of the proto-historic and early historic periods in the southern Levant* (eds. V. Roux and S. Rosen), 157–78, De Boccard, Paris.

Berranger, M., and Fluzin, P., 2012, From raw iron to semi-product: quality and circulation of materials during the Iron Age in France, *Archaeometry*, **54**, 664–84.

Crew, P., 1991, The experimental production of prehistoric bar iron, *Journal of the Historical Metallurgy Society*, **25**, 21–36.

Crew, P., and Crew, S., 1994, The expérimental production of bar iron, in *La sidérurgie ancienne de l'Est de la France dans son contexte européen. Archéologie et archéométrie Colloque de Besançon* (ed. M. Mangin), 175–6, Les Belles Lettres, Paris.

Crew, P., Crew, S., Gilmour, B., and Urteaga, M., 1997, Split blooms and pointed bars from the Ria Oria wreck—trade iron from the Basque Country, in *Early ironworking in Europe: archaeology and experiment. Abstracts of an international conference Symposium, Plas Tan y Bwlch, 19–25 September 1997* (eds. P. Crew and S. Crew), 100–1, Snowdonia National Park, Blaenau Ffestiniog.

Dillmann, P., and L'Héritier, M., 2007, Slag inclusion analyses for studying ferrous alloys employed in French medieval buildings: supply of materials and diffusion of smelting processes, *Journal of Archaeological Science*, **34**, 1810–23.

Dillmann, P., Fluzin, P., and Urteaga, M., 1997, Refining of an experimental Biscaian bloom from Agorregi, in *Early ironworking in Europe: archaeology and experiment. Abstracts of an international conference Symposium, Plas Tan y Bwlch, 19–25 September 1997* (eds. P. Crew and S. Crew), 73–5, Snowdonia National Park, Blaenau Ffestiniog.

Einecke, G., 1950, *Die Eisenerzvorräte der Welt und der Anteil der Verbraucher- und Lieferländer an deren Verwertung*, Stahleisen, Düsseldorf.

Ellenblum, R., 2001, Frankish and Muslim siege warfare and the construction of Frankish concentric castles, in *Dei gesta per Francos: etudes sur les croisades dédiées a Jean Richard, Crusade studies in honour of Jean Richard* (eds. J. Balard, J. Riley-Smith and B. Z. Kedar), 211–22, Ashgate, Aldershot.

Fluzin, P., 2001, Apport de l'archéométrie à la restitution de la chaîne opératoire en sidérurgie; matériaux et procédés. Etudes métallographiques, in *L'obtentcio del ferro pel procediment directe entre els segles IV i XIX. Actes del 6é curs d'arqueologia d'Andorra*, 388–9, Govern D'Andorra, Ministeri de Cultura, Andorra.

14754754, 2015, 3, Downloaded from https://onlinelibrary.wiley.com/doi/10.1111/arcm.12077 by Hanshin University, Wiley Online Library on [31/03/2026]. See the Terms and Conditions (https://onlinelibrary.wiley.com/terms-and-conditions) on Wiley Online Library for rules of use; OA articles are governed by the applicable Creative Commons License

Fluzin, P., 2002, La *chaîne opératoire* en sidérurgie: matériaux archéologiques et procédés. Apport des études métallographiques, in *Aux origines de la métallurgie du fer en Afrique: une ancienneté méconnue* (ed. H. Bocoum), 59–91, UNESCO, Paris.

Fluzin, P., and Leclere, D., 1998, Etat de l'interprétation des scories sidérurgiques à partir d'investigations métallographiques, in *Les métaux antiques: travail et restauration. Actes du colloque de Poitiers* (eds. G. Nicolini and N. Dieudonne-Glad), 135–44, Monique Mergoil, Montagnac.

France-Lanord, A., 1963, Les lingots de fer protohistoriques, *Revue d'histoire de la sidérurgie*, **IV**, 167–78.

Galili, E., and Rosen, B., 2008a, Fishing gear from a 7th-century shipwreck off Dor, Israel, *International Journal of Nautical Archaeology*, **37**, 67–76.

Galili, E., and Rosen, B., 2008b, Marine archaeology in Israel—recent discoveries, *The New Encyclopedia of Archaeological Excavations in The Holy Land*, **5**, 1925–34.

Galili, E., and Sharvit, J., 1999a, Haifa, underwater surveys, *Hadashot Arkheologiyot*, **110**, 15–20.

Galili, E., and Sharvit, J., 1999b, Underwater survey in the Mediterranean Sea 1992–1996, *Excavations and Surveys in Israel*, **19**, 96–101.

Galili, E., Rosen, B., and Sharvit, J., 2002, Fishing-gear sinkers recovered from an underwater wreckage site, off the Carmel coast, Israel, *International Journal of Nautical Archaeology*, **31**(2), 182–201.

Galili, E., Rosen, B., and Sharvit, Y., 2007, Ship assemblages from the southern anchorage of Dor, *Hadashot Arkheologiyot*, **119**, n.p.

Galili, E., Rosen, B., and Sharvit, J., 2010, Artifact assemblage recovered from a Roman shipwreck off the Carmel coast, Israel, *Atiqot*, **63**, 61–110.

Inalcik, H., 1960, Bursa and the commerce of the Levant, *Journal of the Economic and Social History of the Orient*, **3**, 131–47.

Ingo, G., M., and Scoppio, L., 1992, Small-area XPS and XAES study of early iron metallurgy slags, *Surface and Interface Analyses*, **18**, 551–4.

Jacoby, D., 2001, The supply of war materials to Egypt in the Crusader period. *Jerusalem Studies in Arabic and Islam*, **25**, 102–32.

Kapitan, G., 1984, Ancient anchors, technology and classification, *International Journal of Nautical Archaeology*, **13**, 42–60.

Kedar, B. Z., 2012, Prolegomena to a world history of harbour and river chains, in *Shipping, trade and crusade in the medieval Mediterranean: studies in honour of John Pryor* (eds. R. Gertwagen and E. Jeffreys), 5–37, Ashgate, Farnham.

Kleeman, O., 1961, Stand derarchaölogischen Forschung über die eisernen Doppelpyramiden-(spitz) barren, *Archiv für das Eisenhüttenwesen*, **32**, 581–5.

Leroy, S., Cohen, S. X., Verna, C., Gratuze, B., Tereygol, F., Fluzin, P., Bertrsnd, L., and Dillmann, P., 2012, The medieval iron market in Ariège (France): multidisciplinary analytical approach and multivariate analyses, *Journal of Archaeological Science*, **39**, 1080–93.

Mangin, M., 2004, *Le fer*, Errance, Paris.

Pagès, G., Dillmann, P., Fluzin, P., and Long, L., 2011, A study of the Roman iron bars of Saintes-Maries-de-la-Mer (Bouches-du-Rhône, France): a proposal for a comprehensive metallographic approach, *Journal of Archaeological Science*, **38**, 1234–52.

Pagès, G., Long, L., Fluzin, P., and Dillann, P., 2008, Réseaux de production et standards de commercialisation du fer antique en méditerranée: les demi-produits des épaves romaines des Saintes-Maries-de-la-Mer (Bouches-du-Rhône, France), *Revue archéologique de Narbonnaise*, **41**, 261–83.

Pleiner, R., and Bjorkman, J.-K., 1974, The Assyrian Iron Age: the history of iron in the Assyrian civilization, *Proceedings of the American Philosophical Society*, **118**, 283–313.

Redford, S., 2012, A twelfth century iron workshop at Kinet, Turkey. *Byzas*, **15**, 385–92.

Rohrlich, V., Metzer, A., and Zohar, E., 1980, Potential iron ores in the Lower Cretaceous of Israel and their origin, *Israel Journal of Earth Sciences*, **29**, 73–80.

Ronen, A., and Olami, Y., 1978, *Atlit map*, The Israel Archaeological Survey, Jerusalem.

Sauder, L., and Williams, S., 2002, A practical treatise on the smelting and smithing of bloomery iron, *Historical Metallurgy*, **36**, 122–31.

Serneels, V., 1998, La chaîne opératoire de la sidérurgie ancienne, in *Recherche sur l'économie du fer en Méditerranée nord-occidentale* (eds. M. Feugere and V. Serneels) 7–44, Monique Mergoil, Montagnac.

Sprandel, R., 1970, Le commerce du fer en Méditerranée orientale au Moyen âge, in *Sociétés et compagnies de commerce en Orient et dans l'Océan Indien* (ed. M. Mollat), 387–92, SEVPEN, Paris.

14754754, 2015, 3, Downloaded from https://onlinelibrary.wiley.com/doi/10.1111/arcm.12077 by Hanshin University, Wiley Online Library on [31/03/2026]. See the Terms and Conditions (https://onlinelibrary.wiley.com/terms-and-conditions) on Wiley Online Library for rules of use; OA articles are governed by the applicable Creative Commons License

Stantchev, S. K., 2009, *Embargo: the origin of an idea and the implications of a policy in Europe and the Mediterranean, ca. 1100–ca. 1500*, Ph.D. thesis, University of Michigan.
Syon, D., and Galili, E., 2009, Byzantine-period bronze coins from the sea at Dor, *'Atiqot*, **61**, 81–94.

APPENDIX: THE ARCHAEOMETRIC PROTOCOL

The analytical protocol of the sample study is as follows:

- external morphological description and measurements (dimensions and weight);
- photography of each side;
- cutting with lubricant transversally;
- photographs of each cut surface;
- drawings of each cut surface as represented in the metallographic photographs;
- coating in an epoxy resin;
- mechanic polishing with lubricant to a grain size of 1 μm;
- integral observation under a metallographic microscope (magnification between 5 and 50) and characteristic micrographic photos;
- chemical etching with Nital (3% nitric acid in alcohol);
- new integral observation under microscope and characteristic micrographs shots;
- second mechanic polishing with lubricant to a grain size of 1 μm, to eliminate etching effects;
- major element analysis of slag inclusions with a EDS coupled to a SEM:
  – an elemental map is performed with a resolution of 512×512 pixels; each pixel represents a spectrum of 15 ms;
  – on the basis of particle analyses, inclusions are reconstructed by auditioning of the spectrum; particles with fewer than 30 pixels are excluded (450 ms).

SUPPORTING INFORMATION

Additional Supporting Information may be found in the online version of this article at the publisher's web-site:

Supplementary material

14754754, 2015, 3, Downloaded from https://onlinelibrary.wiley.com/doi/10.1111/arcm.12077 by Hanshin University, Wiley Online Library on [31/03/2026]. See the Terms and Conditions (https://onlinelibrary.wiley.com/terms-and-conditions) on Wiley Online Library for rules of use; OA articles are governed by the applicable Creative Commons License